NEGATIVE DIFFERENTIAL RESISTANCE IN HYDRATED DEOXYRIBONUCLEIC ACID THIN FILMS MEDIATED BY DIFFUSION-LIMITED REDOX REACTION

by

HOU KUAN LEE

Presented to the Faculty of the Graduate School of

The University of Texas at Arlington in Partial Fulfillment

of the Requirements

for the Degree of

MASTER OF SCIENCE IN MATERIALS SCIENCE AND ENGINEERING

THE UNIVERSITY OF TEXAS AT ARLINGTON

December 2009

ACKNOWLEDGEMENTS

Sincerely thank Dr. Pranesh Aswath and Dr. Fuqiang Liu for being my committee membere. I would also like to thank Dr. Michael Jin for guiding me from zero to what I have become. I express my egratitude to all the professors in the Department of Material Science and Engineering for offering their knowledge and support. I appreciate departmental administrative assistants; Jennifer Standlee and Lidia Cuauhtli for their helping me go through various paper works and graduation process.

I appreciate Dr. Dong-Chan Shin from Chosun University in South Korea for giving valuable suggestions during his visiting year. I am grateful for all the Nanofab staffs who trained me on various equipments and assistance in the facilities. I feel grateful having the help from my colleagues and all the friends during my thesis work. I thank my group members, Dr. Dong Gun Lim, Dr. Ki-Hyun Kim, Dr. Jong Kwan Lee, Ammena, Soo Kim, Shenbin Wu, Xin Wang, Yi Yang, and Alex Alphonse for a great cooperation and assistance.

I really appreciate Chien-wen Huang for advices about DNA processing programs and sharing the tools. I thank Liang-Chieh Ma for teaching the operation of several equipments and offering valuable advices. In addition, I would like to mention Dr. Hao's group members, Shih-Hsin Chang, Chien-Wen Huang, Punnapob Punnakitikashem, and Yi-Jiun Li. We share the same lab and they generously offered their resources. I have enjoyed the atmosphere we have created together – I felt like we are all in the same group. I also thank my friends, Zi Jing Lin and Yi-Ting Tsai for their assistance with working with computer software.

Finally, I show my greatest appreciation to my parents and my relatives for their love and encouragement.

October 30, 2009

ABSTRACT

NEGATIVE DIFFERENTIAL RESISTANCE IN HYDRATED
DEOXYRIBONUCLEIC ACID THIN FILMS MEDIATED
BY DIFFUSION-LIMITED REDOX REACTION

Hou Kuan Lee, MS

The University of Texas at Arlington, 2009

Supervising Professor: Michael Jin

The charge transport mechanisms in DNA proposed in the literature cover broad range of possibilities including molecular band conduction, superexchange, multistep hole hopping, and polaron hopping. The reason for the surprisingly diverse results is all the variables in the experiments - DNA sequence, DNA characteristic (single molecule or bundle, DNA length), the metal/DNA contacts, and the environmental dissimilarities in temperature, humidity, etc.

In this study, the humidity effect on the electrical conduction in DNA was systematically investigated in a humidity chamber over the wide range of DC voltage. The exponential increase in conduction with increasing humidity was observed for the natural DNA thin-film, and it was attributed to the protonic conduction by the electrolysis of water. In addition, the negative differential resistance was measured in highly hydrated DNA films. The detailed analysis revealed that it was caused by the slow diffusion of water molecules on the surface of DNA molecules.

TABLE OF CONTENTS

LIST OF ILLUSTRATIONS

Figure Page

LIST OF TABLES

CHAPTER 1

INTRODUCTION

1.1 Introduction to This Study

Since molecular structure of deoxyribose nucleic acid (DNA) was discovered by Watson and Crick in 1953 [2], this genetic molecule has had people's attention in both biology and engineering. About a decade ago, people also found out DNA molecules are electrically conducting allowing them to be used in electronic devices[3] and motivating people to investigate the fundamental electrical properties of DNA. Although many numbers of experiments and theoretical calculations have been carried out on various forms of DNA, there is no clear agreement particularly for the long-range electrical conduction of DNA yet. The experimental results covered all the possibilities ranging from an insulator [4] to semiconductor [5], and a superconductor [6]. Among several charge transport (CT) mechanisms proposed - molecular band [5], superexchange [7], mutistep hole hopping [8], phonon-assisted polaron hopping [9], and polaron drift [10], it is generally believed that the hopping mechanism dominates in the long-range conduction of natural DNA predicting very low conduction. Yet, appreciable amount of conduction has been observed from the micro/macro-scale DNA samples and it has been mostly explained by the effect of environments including humidity [11] [12] [13] or by the conduction of counterions in the DNA chains [14]. In this study, the electrical conductance of DNA thin film was systematically investigated as a function of relative humidity and its contribution to the conductance was indirectly proved by experimentally observed negative differential resistance (NDR) in highly hydrated natural DNA thin film samples. The protonic conduction in DNA and NDR is explained by a self-ionized water conduction mechanism and the limited diffusion of water molecules on the surface of DNA chains during its redox reaction respectively. A similar experiment with less hydrophilic DNA-ligand complex thin

film further confirmed the protonic conduction associated with water molecules, which was also concluded by some research groups but without clear evidence.

1.2 Structure of DNA

DNA's double-strand helical structure was discovered by James D. Watson and Francis Crick in 1953 [2], and first drafted by Crick (Figure 1.1(a)). The width between the two strands is about 2.2 ~ 2.6 nm while the distance between base pairs is about 3.3 Å [15]. Figure 1.1(b) shows that the backbones have an 'anti-parallel' direction and the overall shape is similar to a twisted towel. The backbones form two kinds of grooves (Figure 1.1(b)) - one has a longer length and it is called 'major' groove while another with a shorter length is called 'minor' groove.

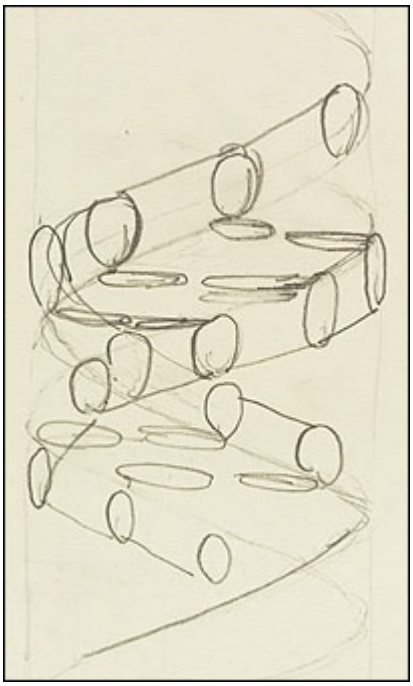

(a)

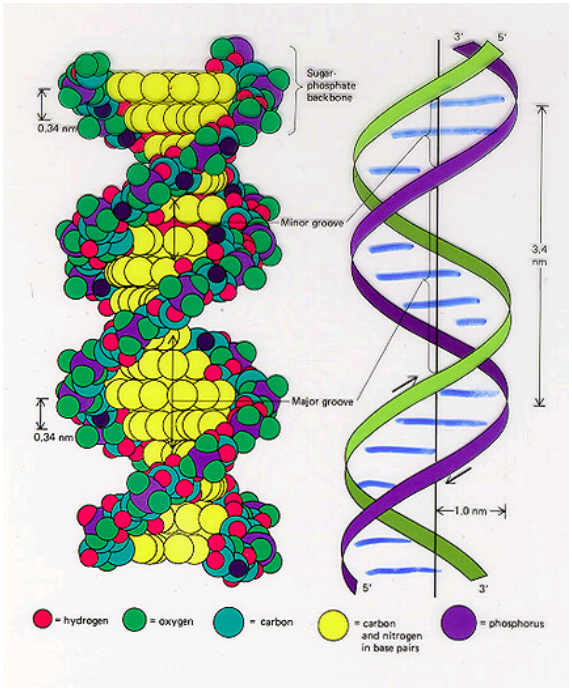

(b)

Figure 1.1: (a) The first draft of double-strand DNA molecular structure made by Francis Crick [16]. (b) Full description figures of DNA double helix structure [17]

The two helix strands are bonded together by a base pair in between the backbones to form a ladder-like structure and there are four different kinds of bases that could form a pair.

The four bases include adenine (A), guanine (G), thymine (T), and cytosine (C) (Figure 1.2), and adenine can only bond to thymine and cytosine can only bond to guanine via hydrogen bonding to form A-T and G-C base pairs respectively (Figure 1.3). The C-G base pair contains three hydrogen bonds while A-T has two. The sequence of DNA - the order of A-T and C-G base pairs in z-direction of DNA molecule -holds the genetic information and involves in protein producing mechanism.

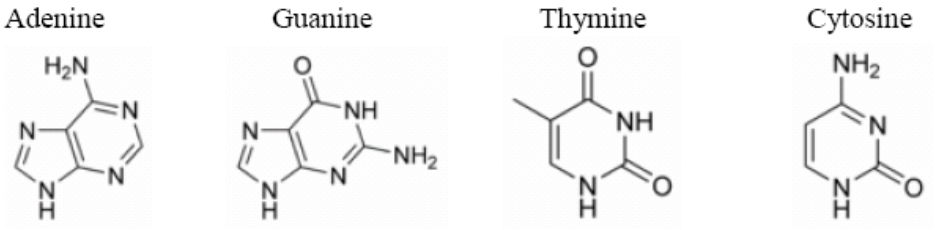

Figure 1.2: Structure of the four different bases in DNA [18].

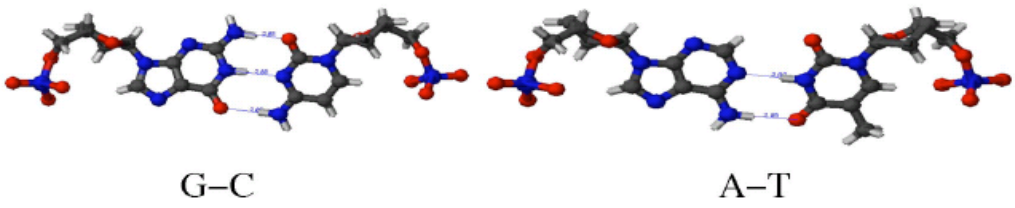

Figure 1.3: The two posible base pairs in DNA (include the phosphate and bases). (C) base is bond to (C) by three hydrogen bonds, while (A) base bond to (T) by two hydrogen bonds. Red color is oxygen atoms and blue color indicates phosphate (outside) and nitrogen (inside bases) atoms [19].

The backbone is made of sugar, a pentose (five-carbon), and phosphate. The sugars are linked together by phosphate groups. In general, a base linked to a sugar ring is called a nucleoside and a nucleoside linked to phosphate groups is called a nucleotide. Figure 1.4 shows the detailed picture of the four bases that connect to the sugar and phosphate backbone forming the nucleotides. One DNA strand always has two different endings: the end with a phosphate group is called 5’ end while the end with a hydroxyl group is called 3’ end. In double

stranded DNA, 5' end from one strand is always paired with a 3' end from another strand and vice versa.

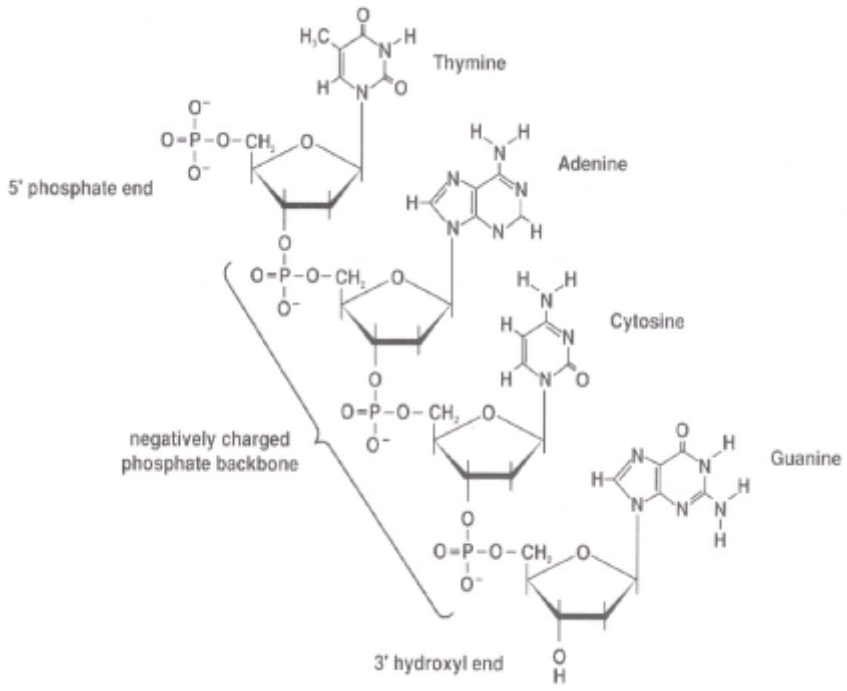

Figure 1.4: The structure of four nucleotides in DNA [20].

1.3 Charge Transport Mechanisms in DNA

DNA is an one-dimensional organic polymeric material system that is a suitable as a model system to help understand the charge transport in disordered materials. For example, the natural DNA can be considered as 'disordered' by having different base pairs sequenced in a random fashion in the molecule. The discussion in this section will start from the fundamental principles of the charge transport (CT) in generalized disordered system and the basics will be applied to DNA. Later, the electronic conduction in the molecular band of DNA will be introduced as another extreme mechanism of conduction in DNA. In addition, the literature review on the conductivity measurements of DNA will be provided.

1.3.1 Electronic Charge Transport Mechanisms in Disorder Systems

Figure 1.5 shows a typical density of states versus energy curve from a disordered solid system. ε_c is called mobility edge which separates the extended states from the localized states.

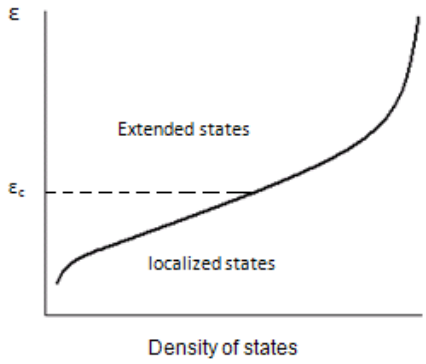

Figure 1.5: Density states in a disordered solid system. ε_c is the mobility edge that separates extended states and localized states [21].

Electrons in the extended states can freely move and contribute to the electrical conduction. However, in a highly disordered system, CT via extended states is less possible because each electron energy state tends to be independent and it becomes more localized (Anderson localization [22]). The degree of localization in different disordered systems is often depicted by a delocalization length, α. The smaller α is, the more localized the system is. Mott has contributed massively to CT mechanisms in disordered systems and readers can find more information in his publications [23] [24] [25], and suggested that hopping between the localized states should be the primary mechanism of CT in highly disordered systems. The hopping mechanism can be divided into two catalogs: nearest neighbor hopping (NNH) and variable range hopping (VRH). Details will be discussed in the following sections.

1.3.2 Hopping From One Electronic State to Another

The hopping mechanism is a tunneling transition between two localized and discrete states. A tunneling transition probability (V_{ij}) of a hopping from a localized state, i to another lower energy state, j, is defined by the equation (1.1),

$V_{ij} = V_0 \exp(-2r_{ij}/\alpha)$ (1.1)

where r_{ij} is the spatial distance between two jump sites, and α is the localization length [22]. The magnitude of the coefficient, V_0 depends on the electronic interaction mechanism that causes the transition. In disorder systems, the transition is dramatically affected by phonons, which can be told by the fact that the experimental V_0 value is similar to phonon frequency [26].

If hopping occurs from lower energy state, ε_i to a higher energy state, ε_j as shown in Figure 1.6, the transition rate should also depend on the energy difference, $(\varepsilon_i - \varepsilon_j)$ and temperature [27]. As a result, (1.1) is modified to equation (1.2),

$V_{ij} = V_0 \exp(-2r_{ij}/\alpha) \exp(-|\varepsilon_i - \varepsilon_j|/2kT)$. (1.2)

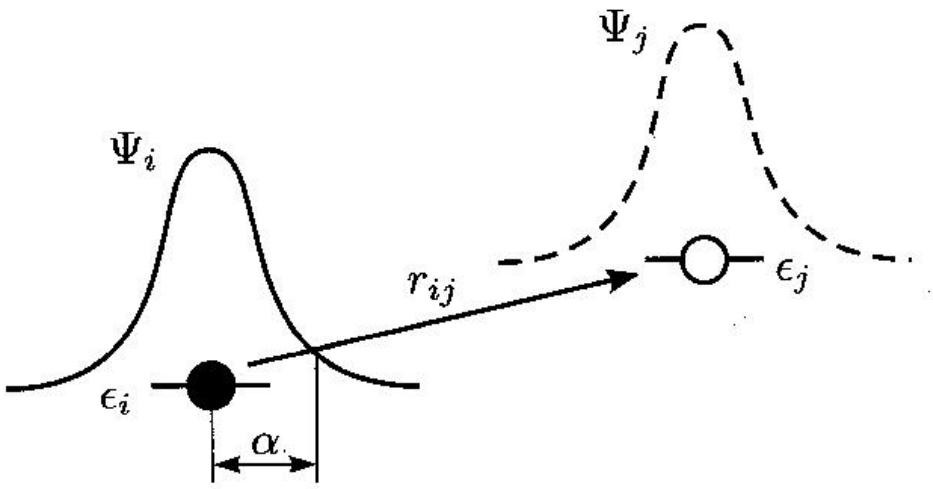

Figure 1.6: Hopping from a lower energy state, ε_i to a higher energy state, ε_i. ψ_i and ψ_j are their Bloch wavefunctions. r_{ij} is the spatial distance between two jump sites, and α is the localization length [25].

Both equations, (1.1) and (1.2) are based on the assumption that i state is occupied but j state is empty, so it is necessary to include the energy distribution of electrons using Fermi-Dirac distribution function for the complete equation. The final equation is written as (1.3),

$V_{ij}=V_0\exp(-2r_{ij}/\alpha) \exp\{-(|\varepsilon_i - \varepsilon_j| + |\varepsilon_i - \varepsilon_f| + |\varepsilon_j - \varepsilon_f|)/2kT\}$, (1.3)

where ε_f is Fermi energy. With the formula, the electrical conductivity can be calculated as shown in appendix A.

1.3.3 Nearest-Neighbor Hopping (NNH) Mechanism

Assuming the localized states in a disordered system are separated out in random distances, the electrons will choose the easiest path to conduct. When the temperature is high, the carriers will get enough thermal energy to overcome the potential barriers of vicinity states and the first exponential term in the equation (1.3) becomes the limiting factor in CT. Accordingly the hopping rate increases with a decreasing r_{ij}. Carriers will find an efficient path to transport through the system, therefore they will hop to a nearest neighbor site which is known as NNH. This case can only happen at relative high temperature - the threshold temperature will vary because different materials have different localization length and tunneling coefficient (V_0).

1.3.4 Variable Range Hopping (VRH) Mechanism

The concept of variable range hopping was first discussed by Mott [25]. He argued that, if the temperature is low enough, the carriers cannot get enough thermal energy to overcome the potential barriers of vicinity states and jump to states in a distance with a lower energy barrier - variable range hopping (VRH). In other words, the second exponential term (energy-dependent term) of the equation (1.3) will limit the hopping rate. Consequently, VRH typically has lower conductivity than NNH. The conductivities derived from both NNH and VRH is present in Appendix B.

1.4 Charge Transport Mechanisms in DNA

The charge transport in DNA has been extensively studied in the field of both molecular biology and electronics for its potential in various bioengineering applications [28]. Since the first measurement of the electrical conduction properties of DNA by Duchesne *et al.* in 1960 [29], a number of studies have been carried out and proposed various conduction mechanisms including molecular band conduction [5], superexchange [30], hole hopping [30], and phonon-assisted polaron-like hopping [11]. Long-range electrical conduction of DNA can be supported

by molecular band, which has been explained by the π-conjugation between base pairs along the z-direction of DNA. In fact, very high electron transfer rates were measured in a double-stranded poly(G)-poly(C) DNA with 30 base pairs (bps) and 600 nm-long DNA ropes have shown the electrical conductivity comparable to typical conducting polymers [31]. On the other hand, most temperature- and frequency-dependent long-range conductivity experiments on micro/macroscopic DNA samples have suggested that the conduction occurs primarily through hopping mechanisms that are common to charge transport in disordered organic materials [32],[33],[1],[34],[35]. In addition, the study on the effect of base pair structure of DNA indicates long π-conjugation is less favorable in natural DNA with a random sequence of base pairs concluding that DNA is insulating at length scales longer than 40 nm even for the double-stranded poly(G)-poly(C) DNA, with a 10 TΩ lower bound for its resistance.

In the following subsections, various CT mechanisms in DNA will be introduced in details from a molecular band conduction to a polaron hopping mechanism. The hopping mechanisms are based on the CT mechanisms in disorder materials, which have been introduced in the previous section.

1.4.1 Molecular Band Conduction

The mechanism is explained by the overlap of π_Z orbits from base pairs within DNA molecule and the consequent orbital conjugation in z-direction of the DNA strands as shown in Figure 1.7. The red loops are the π_Z orbits and if every neighboring π_Z orbit is sufficiently overlapping to each other, the band will form and the carriers will transport through the core of the DNA molecule.

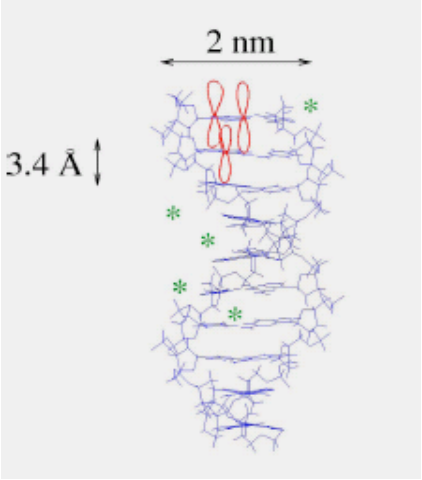

Figure 1.7: A sketch of DNA and its π_Z orbits. Stars are counterions that neutralize the phosphate backbones [20].

If the mechanism dominates the conduction, the electrical conductivity will have no distance-dependence and the transport rate should be fast. The mechanism can possibly explain the high electrical conductivity measured [6] and the high transport rate from semiconducting DNA [5]. It is also consistent with the principle of CT via the extended states discussed in the previous section.

1.4.2 Superexchange and Multi-Step Hole-Hopping

While the π-conjugation in DNA is still a debate, the hopping mechanism is the most probable conduction mechanism to interpret the experimental results. If hopping is the primary conduction mechanism, the conductance will decrease tremendously as a function of the length of DNA chain. From equation (1.3), the hopping distance is directly related to temperature which is confirmed by both experimental results [1, 34] and theoretical calculations [33, 36, 37].

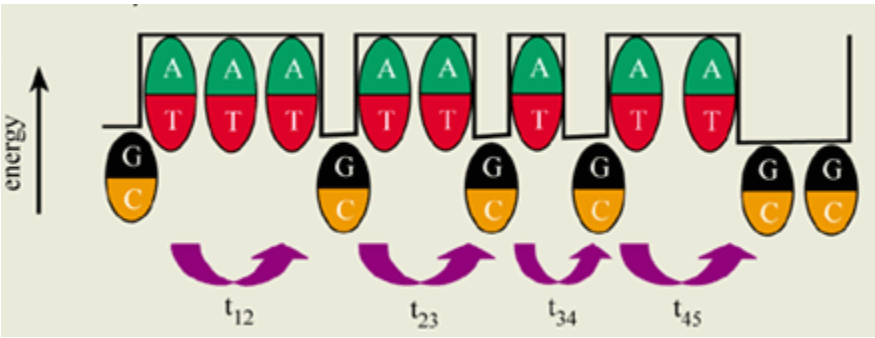

Figure 1.8: Superexchange (or VRH) in DNA [38].

Figure 1.8 presents the superexchange mechanism in DNA. Compared to A-T base pair, C-G pair has smaller oxidation energy so holes prefer to stay at C-G bases. Instead of hopping from C-G base to A-T base, the holes choose to hop from C-G to next C-G base in Z direction. On the other hand, holes hop through the nearest base in the case of multi-step hole hopping mechanism (Figure 1.9). In fact, superexchange is another way to explain VRH in DNA while multi-step hole-hopping depicts NNH mechanism.

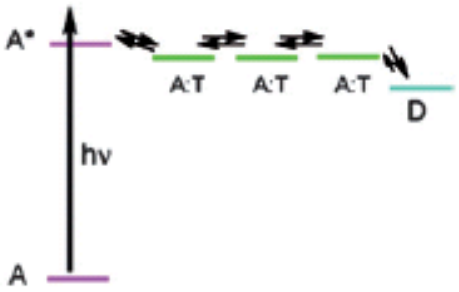

Figure 1.9: Multi-step hole hopping (or NNH) [39].

Figure 1.10 shows the experimental data from Tran *et al.* [1] and theoretical fitting by Yu *et al.* [37]. It is interesting to note that there is a crossover around at temperature 200 ~ 250 K, which indicates the transition between the superexchange and the multi-step hole hopping. At temperatures lower than 200 K, the fitting showed the superexchange (VRH) behavior while at temperatures above 250 K, the fitting suggested the multi-step hole hopping (NNH) mechanism.

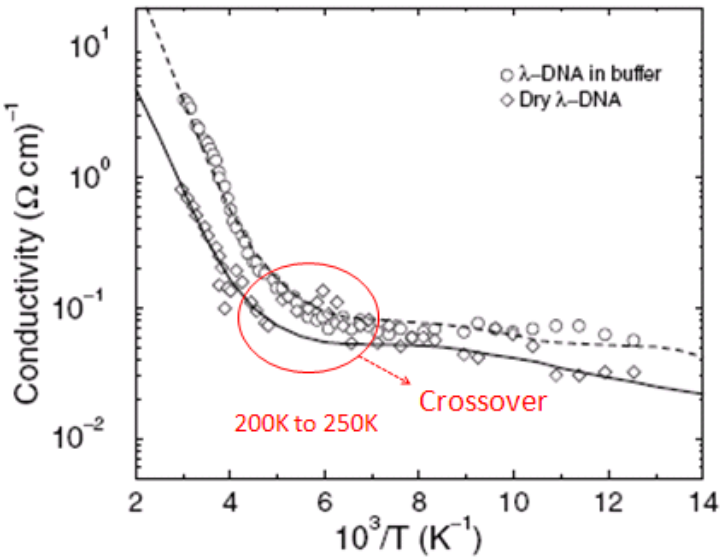

Figure 1.10: Conductivity versus inverse temperature of λ-DNA in buffer solution (circle) and dried λ-DNA (diamond) [1]. The solid and dashed lines are the theoretical fitting by a VRH (T < 200K) and NNH model (T > 250K) [37].

Furthermore, Tran *et al.* obtained the activation energies (E) of 0.15 eV for the dry λ-DNA and 0.165 eV for λ-DNA buffer solution above 250 K according to $\sigma \sim \exp(-E/kT)$ where k is Boltzmann constant [1]. Meanwhile, the conductivity showed very weak temperature dependency below 200 K. This can be understood by the transition from VRH at low temperature to NNR at high temperature.

1.4.3 Phonon-Assisted Polaron Hopping

Gary *et al.* presented a new idea of CT mechanism in 2000 [10]. The report claimed that CT mechanisms include not only superexchange, or discrete energy states hopping but also the phonon-assisted polaron hopping, which should exist in both superexchange and hopping mechanisms. It suggested that DNA is a dynamic molecule, and injecting carriers will cause its structure change. Cations on DNA bases are electron-deficient, so DNA will distort its local structure to relieve this deficiency. The distortion is usually formed by several neighboring DNA bases and the distortion will hop through the DNA chain with the carriers, as shown in

Figure 1.11. The number of bases in a polaron is depending on whichever can achieve minimum Gibbs energy and also it is base sequence-related.

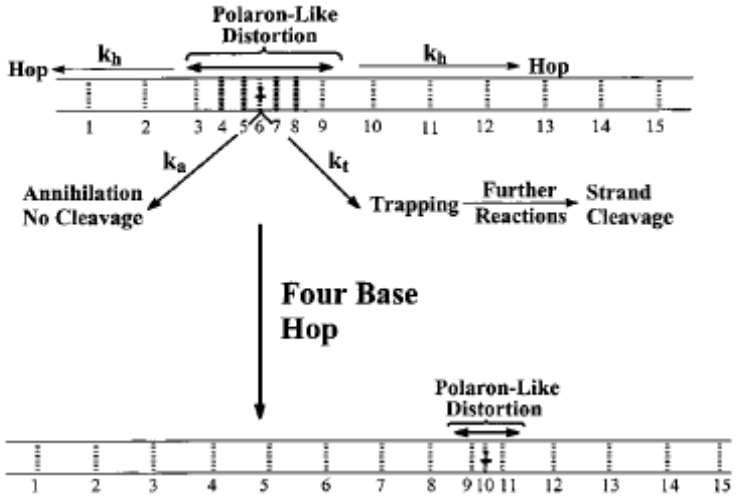

Figure 1.11: Polaron hopping mechanism in DNA [10].

1.5 Review on DNA Conductivity Measurements

The question of whether DNA conducts intrinsically or not is still a debate. The experimental results cover all possibilities, from being an insulator [4],[40], a semiconductor [5],[41], a ohmic-like (linear I-V) behavior [31],[42],[34], to a superconductor [6]. The reason for the inconsistency is all the “variables” present in the experiments. The variables can be separated into three categories. The first is the different metal contacts made to DNA, the second is the characteristics of the specific DNA molecules used, and the third is its surrounding environment during measurements. The following sections will explain the importance of the contacts and the intrinsic characteristics of DNA used in the experiments first and the effect of humidly, which has been considered to be very important in the electrical conduction of DNA, will be discussed in Section1.5.

1.5.1 Contacts

The work function of the metal electrode is important because the energy difference between the work function of the electrode and the energy level of the DNA molecule can create an energy barrier. If free electrons from electrodes have to climb up a big barrier to reach DNA molecule, the overall conductivity of DNA will be limited by the process and the barrier will have rectifying behavior. Therefore, the first important variable is the work function of the electrode metal used. For example, many experimental results have suggested that the work function of Au is slightly larger than the lowest unoccupied molecular orbit (LUMO) of DNA if the LUMO is determined by G base (Figure 1.12). It is also possible to consider the DNA backbone as a contact barrier for the tunneling process of carriers from the electrode directly to the base of DNA. However, it has not been discussed much in the literature how big this barrier would be.

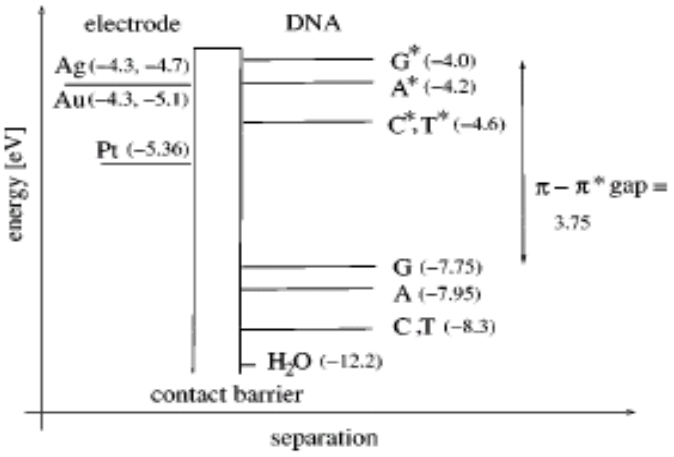

Figure 1.12: Electronic energy levels of bases in DNA and metal electrodes typically used with DNA [19].

1.5.2 Characteristics of the DNA as a sample

(1) Base sequence in DNA: Since each base has their own highest occupied molecular orbit (HOMO) and LUMO (Figure 1.12), DNA will show different conductivity if the sequence of base pairs are different. Filoramo *et al.* found out that the more C-G base pairs the DNA had, the higher the conductivity was [43].

(2) Length of the DNA: The conjugation length in nature λ-DNA with a random base pair sequence is about 40 nm, and showed a behavior of an insulator if the length of DNA becomes longer than that [4].

(3) Types of DNA: Single DNA molecular chain versus micro/macro-scale of DNA samples including a DNA rope, network DNA, and thick and long planar films. In addition, there are various polymorphs in DNA [26].

(4) Counterions and ligands attached to the backbone of DNA: Various counter ions and ligands are possible for natural and synthesized DNAs. The ionic conduction by the counterions has been studied [45]. Further discussion will be made in the following sections.

1.5.3 Survey of Experimental Results

Most studies made so far usually define insulator, semiconductor, conductor, and superconductor based on the magnitude of the resistivity of DNA. The insulator has the highest resistivity while that of superconductor approaches zero. The outcome from the DNA conductivity measurements has shown all the possible cases and the following sections summarize the findings.

Case 1: Insulator

Storm and his co-workers did a series of measurements (Figure 1.13) they varies the sequence of base pairs DNA, the metal electrodes used (Pt and Au), and studied both single molecule and bundle DNA molecules [4]. All devices showed no conduction up to 10 V, and the result was confirmed by Zhang and his co-workers later [44].

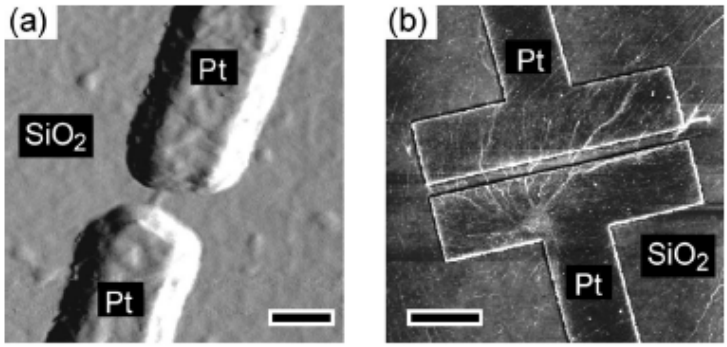

Figure 1.13: AFM pictures of different electrodes and gap distances used in Storm *et al.* [4]:(a) A single molecule of natural λ-DNA was trapped between Pt electrodes. The gap between the electrodes was 40 nm gap and the scale bar in the figure is 50 nm, (b) poly(G)-(C) DNA boundless placed in a 200 nm wide gap created by Pt electrodes. (scale bar: 1 μm).

Case 2: Semiconductor

Porath and his co-workers [5] measure the direct conductivity using a 10.4 nm long DNA containing only poly(G) - poly(C) base pairs (30 base pairs), and found that the I-V curve showed a gap in voltage (flat area with no current) with a magnitude of about 1 ~ 2 V [Figure 1.14 (a)], which was attributed to the difference between the work function of Pt electrode and LUMO level of a molecular band formed by DNA bases. They also suggested that there is a π conjugation throughout the DNA molecule because of the electron transferring rate is extremely high. The study by Rakitin *et al.* [41] also showed similar results. They prepared 15 μm-long natural λ-DNA and metal-doped DNA, and observed the similar gap in voltage as Porath group showed in their I-V curves [Figure 1.14 (b)]. However, the current is supposed to be lower if the length of DNA matters, but similar current was measured, which needs yet to be answered. Nonetheless, a π_z band structure was also suggested in Rakitin's work.

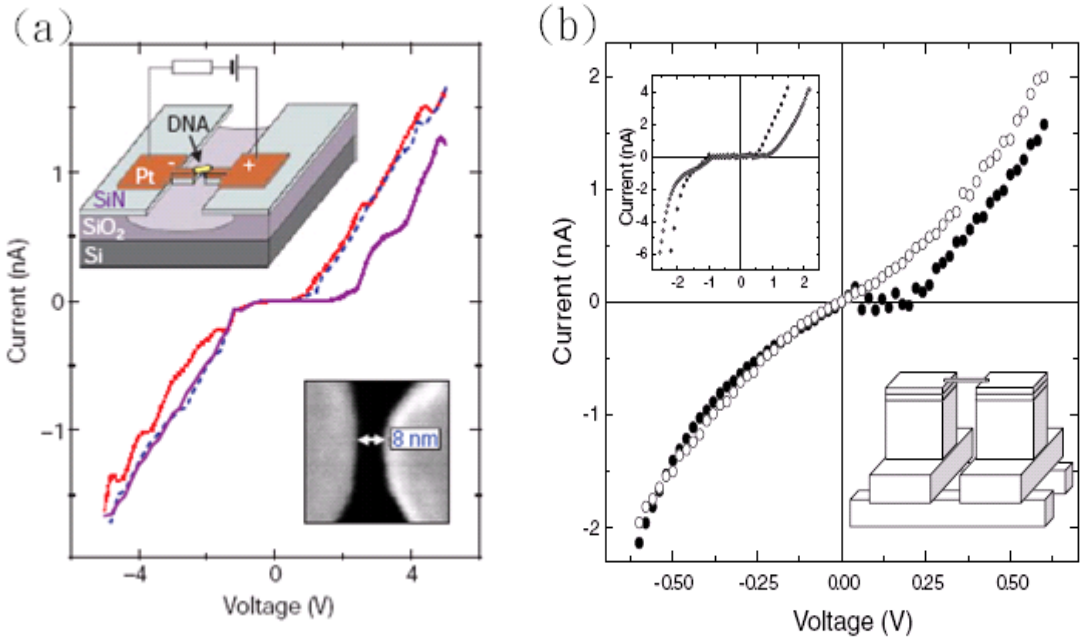

Figure 1.14: (a) I-V curves at room temperature by Porath *et al.* Line curves with different colors indicate multiple measurements with the same sample. All of them showed a gap in voltage with different magnitude, which was attributed to the humidity in the air was not constant [5]. (b) I-V curve obtained by Rakitin *et al.* Open circle is M-DNA (imino groups in the base pairs replaced by metal ions) and closed circle is 15 μm-long natural DNA. The gap between Au electrodes was 10 μm [41].

Case 3: Ohmic or Nearly Ohmic

Yoo *et al.* studied poly(G)-poly(C) and poly(A)-poly(T) DNA bundles each made with about 300 molecules of DNA by trapping them between either Au or Ti electrodes (Figure 1.15) [34]. Both poly(A)-(T) and poly(G)-(C) DNAs in Figure 1.15 show an ohmic behavior at room temperature and the reason for being ohmic was ascribed to the linear nature of hopping mechanism Tran *et al.* used the non-contact microwave cavity absorption method to measure conductivity instead of using metal electrodes in order to get more reliable results because any issue with the metal contact can be ignored and to achieve ohmic [1]. In additioin, they studied DNA ropes in dry and buffer-solution conditions. It confirmed that the B-form of DNA (polymorph with more water content in the molecule) structure has higher conductivity.

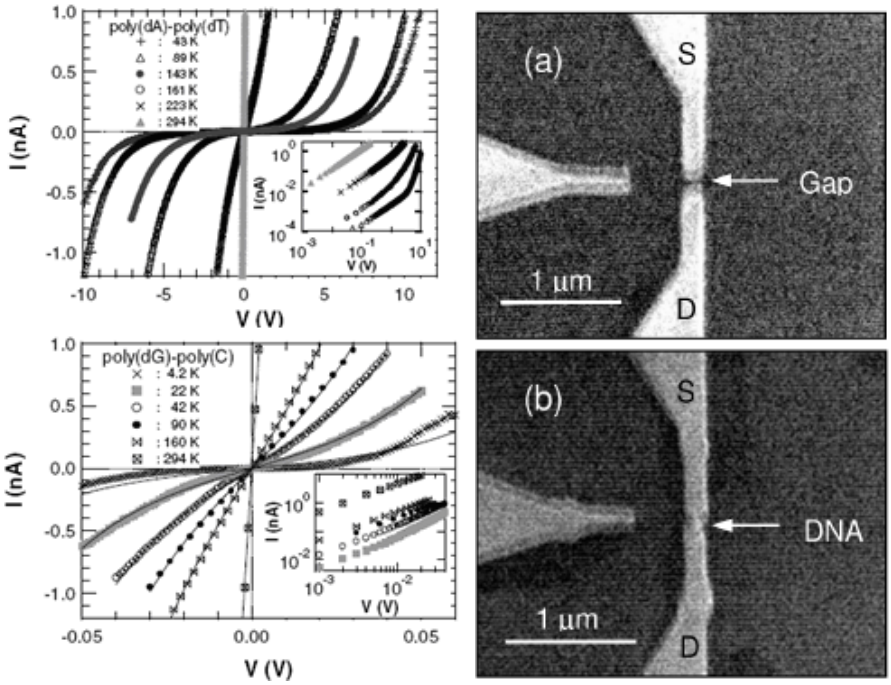

Figure 1.15: (Left) (a) SEM pictures of conductivity experiments by Yoo *et al.*- S and D represents a Au/Ti electrode . The gap between the electrodes is 20 nm wide. (b) DNA is trapped between the electrodes. (Right) I-V curves of poly(A)-(T) (top) and poly(G)-(C) DNA (bottom) with varied temperature under vacuum [34].

Case 4: Superconductor

Kasumov *et al.* [6] deposited double-stranded λ-DNAs on a superconductive rhenium/carbon (Re/C) electrodes with a 500 nm-wide gap. DNA molecules were prepared into three samples; (i) DNA1 - around 10 DNA molecules on the electrodes with 30 µm wide window, (ii) DNA2 - 40 molecules with a 120µm wide window, and (iii) DNA3 - two/three DNA molecules with the same 120µm wide window. At temperature less than 1 K, DNA1 showed superconducting behavior.

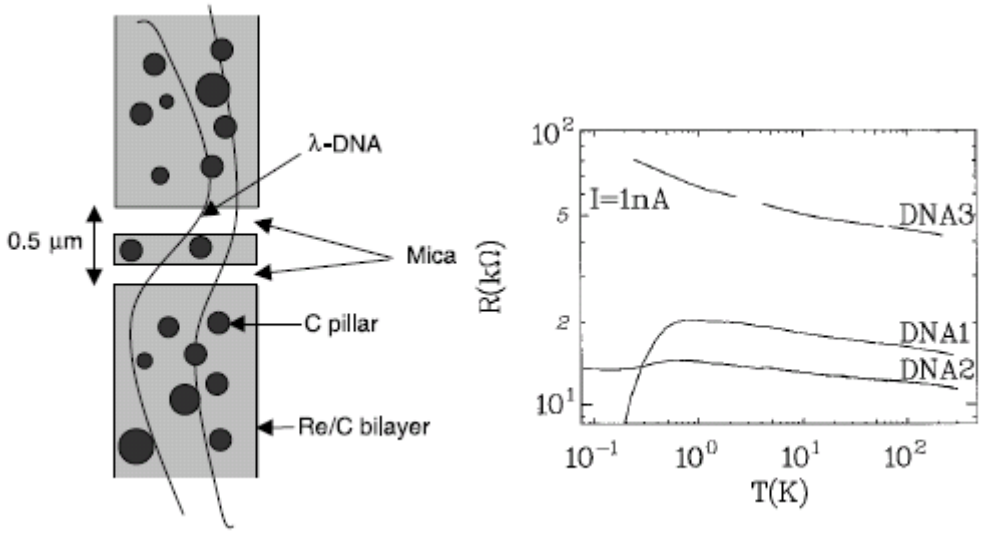

(a) (b)

Figure 1.16: (a) λ-DNA molecules on a Re/C electrodes on a mica substrate with a 0.5 μm-wide gap. (b) DC resistance as a function of temperature of three DNA samples [6].

Table 1 summarizes all the results presented in previous sections. Based on the review, the following conclusions can be made.

1. Compared to the natural DNA that has a random sequence of base pairs, DNA with the same base pairs tend to form a delocalized π band. Rope, bundle and network DNAs are most likely ohmic conductors because hopping is the dominant conduction mechanism as far as there is no molecular band.
2. Poly(G)-poly(C) DNA is more conductive than poly(A)- poly(T) at low temperature where VRH is dominant The reason is poly(G)-poly(C) has a lower oxidation energy than that of poly(A)-poly(T) DNA. Having water in DNA is favor for high conduction.
3. Conduction mechanism can change at different temperature.

Table 1.1: Summary of the DNA Conductivity Measurements from the Literature.

Case	**Group**	**DNA types**	**Electrodes**	**Temperature**	**Gap width**	**Counterion**
1. insulator	Storm *et al.*	DNA molecules buffer solution	Pt and Au	300 K (RT)	40 ~100 nm	Mg^{2+}
	Zhang *et al.*	single DNA molecule	Au	RT	4 μm	
2.semiconductor	Porath *et al.*	single poly(G)-poly(C)	Pt	RT	10.2 nm	Mg^{2+}
	Rakitin *et al.*	single molecule	Au	RT	10 μm	NA^{+}
3.ohmic	Yoo *et al.*	supercoiled poly(G)-poly(C)				
		poly(A)-poly(T) bundles	Au/Ti	RT	20 nm	NA^{+}
	Tran *et al.*	dry and wet bundles	Microwave absorption	80 K ~ RT		NA^{+}
4.superconductor	Kasumov *et al.*	few molecules	Re/C (self-assemble)	T < 1 K	500 nm	Mg^{2+}

1.6 Water Contribute to Conduction

Water contribution to the conductivity of DNA is important because water is not only can change the DNA structure but it is also possible to create hopping channels for ions that could be present in DNA (H^+, OH^-, $H3O^+$, Na^+, K^+, Mg^{2+}, etc.) to conduct. Following subsections will elaborate on the topic.

1.6.1 Water Content and DNA polymorphs

It has been known that DNA with sufficient water content prefers to form B-DNA while dehydration will change the geometry of DNA to A-DNA [45],[46]. Their structures are shown in Figure 1.17 and their structural parameters are summarized in Table 2.

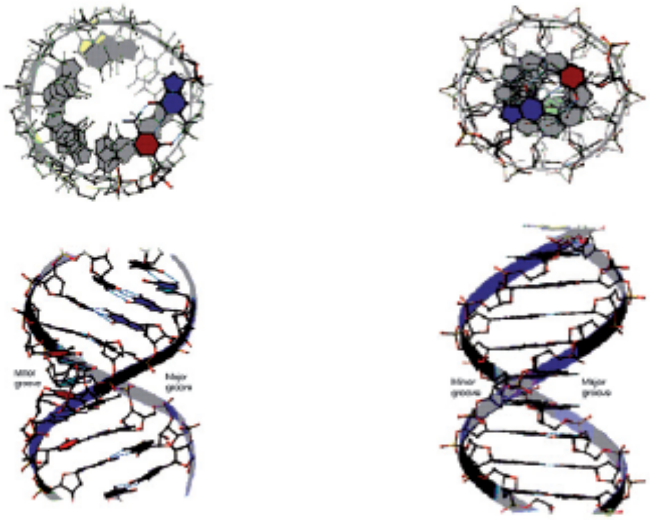

(a) (b)

Figure 1.17: The three-dimensional structure of A-DNA and B-DNA. (a) A-DNA top view (top) and side view (bottom). (b) B-DNA top view and side view [14]

Table 1.2: The Structural Parameters of A-DNA and B-DNA [47].

	A-DNA	B-DNA
Vertical distance between neighboring base pairs	2.55 Å	3.4 Å
Radius of the base pair planes	11.5 Å	10 Å
Numbers of base pairs per turn of helix	11	10
Helix angle between neighboring base pairs	32.7°	36°
Helix rotation direction	Right-handed	Right-handed

It was concluded that 18 to 19 water molecules per nucleotide are needed to be B-DNA and 13 to 15 are required to form A-DNA [48]. A-DNA has less number of water molecules because hydrophobic sugar rings are much more exposed in A-DNA. In addition to humidity, it was also found that the DNA sequence and the type of the counterion around DNA backbones also affect DNA structure [49].

1.6.2 Water in DNA

Very recently Julia *et al.* reported how water affects the electronic properties of DNA base pairs [50],[51]. In Figure 1.18, water molecules attach to A-T and G-C base pairs via hydrogen bonding.

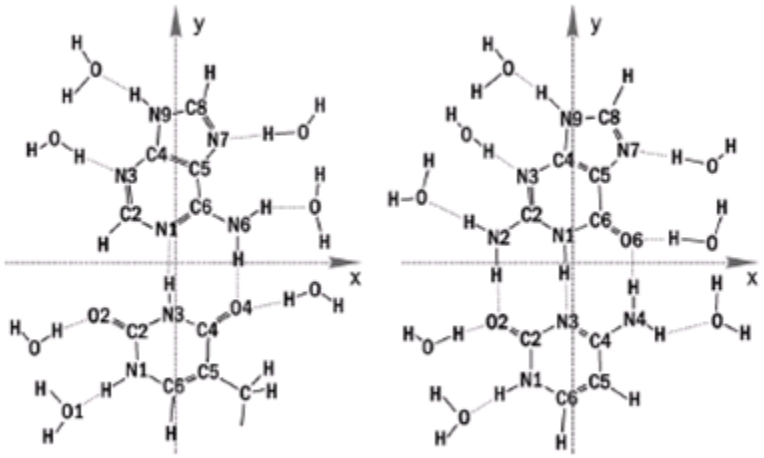

(a) (b)

Figure 1.18: The bonding between water molecules and bases in DNA: (a) A-T base pair and (b) C-G base pair [50].

The result suggests that the bonding between water and DNA base shifts the HOMO level of each base and decrease the potential barrier between G-C and A-T from 0.7 eV to 0.123 eV. Consequently, the CT between two types of bases increases.

Gilbert and his coworkers were the first group presented a water channel structure along the DNA chain [52]. The water molecules bind to the N and O sites in the core of base pairs as shown in Figure 1.18. In Figure 1.19, three dimensional schematic shows the DNA and water coupling. If the hydration is strong and saturates each base, a hydration channel is able to form in the middle of DNA chain.

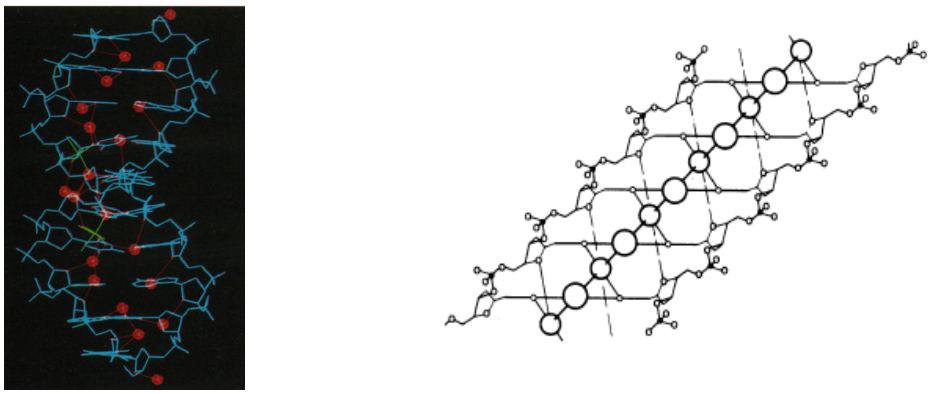

(a) (b)

Figure 1.19: Schematic of the formation of water channel in DNA: (a) water molecules (red sphere) and hydrated counterions (green cross) and (b) water spine (circle in the DNA chain [52].

In 2002, Kawai *et al.* provided more detailed study on binding of water molecules to DNA [12]. According to their infrared spectroscopic data, most water bind to the phosphate groups under 65% relative humidity (5 to 6 water molecules per phosphate group (Figure 1.20). When the humidity is increasing further, water molecules go into bases and bind to amino, imino, and keto groups and they are expected to form a hydration channel as previously explained. When the relative humidity reaches 80% (20 water molecules per base pair), the water molecules start being physically absorbed to neighbor water molecules that are already

bound to DNA and eventually form a water layer around DNA backbones. This has been experimentally agreed by Jo *et al.* [53] and TuuKKanen *et al.* [54].

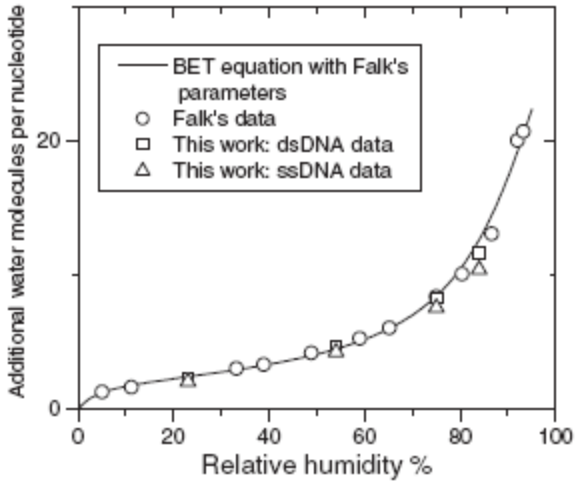

Figure 1.20: Water molecules per nucleotide versus RH (%) [55].

1.6.3 Ionic Conduction in DNA

It has been found that with increasing humidity, the conductivity exponentially raises. The ionic conduction is the most well-accepted answer to explain it. The ionic conduction is proportional to their density, n and mobility, μ [56]. Therefore, with increasing humidity, either carrier density raises or mobility of ions increases. To understand the dominant contribution, it is important to know the type of ions is in charge of the conduction. Apparently increasing hydration could give counterions more mobility and also increase the densities of H^+ and OH^- ions. Ionic conduction needs activation energy as the dissociation potential between the cation and the anion is $E_c = e^2/ (4 \pi \varepsilon_0 r)$ [57], where ε_0 is the dielectric constant in vacuum and r is the distance between the cation and the anion - Ronne *et al.* [58] applied Debye formation [59] to estimate the dielectric constant for the water in DNA.

Ha *et al.* [11] studied the effect of humidity on poly (G)-(C) and poly (A)-(T) DNA conductivity. DNA (around 2μm long) solution was drop-casted onto Au/ Ti nanoelectrodes with

a gap of 200 nm. Then the measurement was carried out in a temperature and humidity controller chamber. The result showed a linear relation between humidity and conductivity at room temperature (Figure 1.21(a)). Secondly, they measured the conductance with temperature range from 330 K to 280K (Figure 1.21(b)), calculated the activation energy to be about 0.5 eV using $\sigma = \sigma_0 \exp(-E/kT)$ [60], and compared the results with their previously measured activation energy of 0.2 eV for DNA in vacuum [34]. They suggested an ionic conduction which is possible by the flow of deionized water ions (hydronium and hydroxyl). However, they could not provide enough information to exclude conduction by counterions.

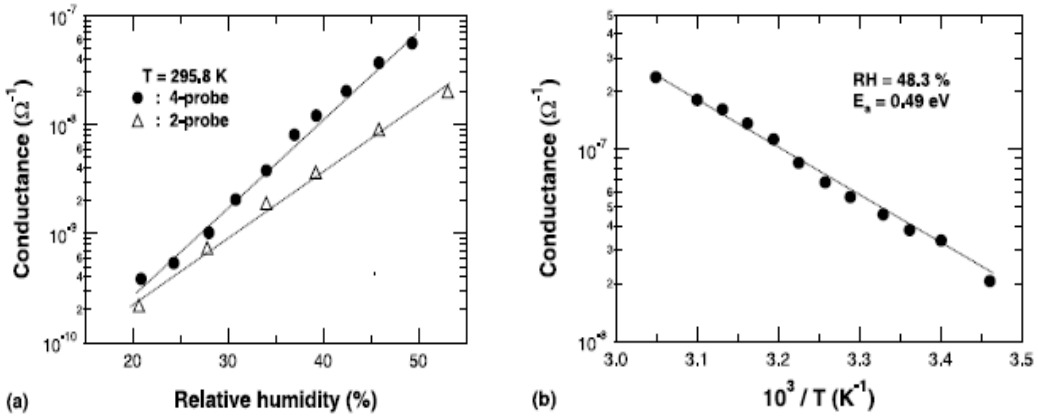

Figure 1.21: Conductance of poly(G)-poly(C) versus (a)versus RH (%) (b) versus temperature [11]. The 4-point probe and 2-point probe methods were used to measure in (a). The difference is given by contact resistance of the probes. The activation energy E_a for the conduction is derived from an equation, $\sigma = \sigma_0 \exp(-E/KT)$.

The ionic conduction in DNA was also observed by Okahata *et al.* [61] and Cai *et al.* [42]. A DNA complex was used in Okahata's experiment by replacing Na counterion with cetyltrimethylammonium (CTMA). They aligned DNA thin film by a uniaxial stretching and measured the resistivity – the DNA complex film was deposited on Au electrodes with a gap of 5 μm at room temperature. Resistivities of 10^5 Ω•cm and 10^9 Ω•cm were found respectively for stretching direction and a direction perpendicular to the stretching – unstretched (unaligned) DNA complex film gave the resistivity of $10^7 \sim 10^8$ Ω•cm.

Most recent experiment was carried out by Kleine *et al.* in 2006 [13]. They used double and single strand DNA to measurement the conductivity as a function of humidity (10% to 100% RH). It showed that the current was exponentially increasing as a function of RH and there was almost no difference of hybridized double-strand DNA and denature single-strand DNA as shown in (Figure 1.22(a)). Then they compared the I-V characteristics of DNA with high RH% to those of different solvents. The results (Figure 1.22(b)) showed that the I-V curve from DNA was similar to that of distilled water concluding Figure 1.22(b) In fact, they pointed out that the increase of current at around 2 to 2.5 V is consistent with the dissociation voltage of water molecule determined by the difference in the electrochemical redox potentials of the two participant half cells, H_e/H_3O^+ and OH^-/ O_2 [21].

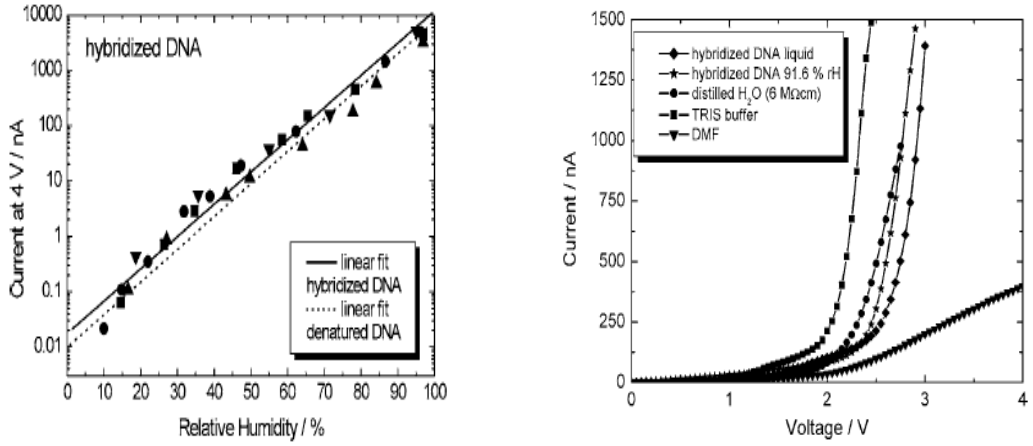

(a) (b)

Figure 1.22: Electrical characteristics of DNA as a function of RH (%): (a) current versus RH% and (b) I-V curve of different samples including pure solvents, distilled water, and two DNA samples [13].

Table 2 compiles the literature results on the temperature dependence of the DNA's conductivity. Often the effect of water was considered and the important findings are summarized as follows.

1. There is a crossover temperature at 200K to 250K that was observed in every group. Therefore the charge transport mechanisms are changing across this temperature.

2. Surrounding environment can hugely influence the charge transport mechanism. Water can offer an ionic conduction channel.
3. Metal-organic contact can create a thermionic emission energy barrier, which limits the conduction.
4. Trend in the activation energies for each mechanism are (i) 0.12 eV for hopping in a single poly(G)-(C) DNA chain in vacuum, (ii) 0.5 to 0.6 eV for ionic conduction, (iii) 0.5 eV to 0.7 eV for thermionic emission, and (iv) 0.7 to 0.9 eV for hopping in micro/macro scale DNA thin film. If the DNA chain length is much shorter than the gap between electrodes, the energy reached 0.9 eV (under vacuum). It may suggest that charges hop between DNA chains.

Table 2: Summary of activation energy for DNA and their suggested charge transport mechanism

Group	DNA (bps)	Prep.	CT	Activation Energy(eV)	Electrodes (Gap, nm)	Temp. (K)	Note	Ions
A&M	Origami (~4,500bps)	drop-casted	hopping	0.7 to 0.9	Pt (100)	240~320	vacuum	Na^{+}
Yoo	A-T (4,000 ~ 5,000)	drop-casted	polaron-hopping	0.18	Au/Ti (20)	RT~20	vacuum	Ca^{2}
	G-C (5,000 ~ 8,600)	drop-casted	Polaron hopping	0.12	Au/Ti (20)	RT~20	vacuum	Ca^{2}
Yoo	A-T (4,000 ~ 5,000)	drop-casted	ionic conduction	0.6	Au/Ti (180)	290~330	ambient	Ca^{2}
	G-C (5,000 ~ 8,600)	drop-casted	hopping (at high T)	0.49	Au/Ti (180)	290~330	ambient	Ca^{2}
Inomata	λ-DNA (48,502)	molecule combing	polaron hopping (at low T)T)	0.21	Pt (200)	20~300	vacuum	Na^{+}
Gullu	human extracted DNA	thin film	thermionic emission	0.54~0.74	Al/InP	80~300	vacuum	Na^{+}
Kutnjak	Li-DNA (15,000)	thick film (20 to 80 μm)	hopping	0.83	Au & Cu	250~310	Ambient (RH75%)	Li^{+}
“	“	“	“	0.98	“	“	vacuum	“

CHAPTER 2

EXPERIMENTS

2.1 DNA and DNA-CTMA Preparation

Salmon DNA purchased from Sigma-Aldrich (USA) was used as received in this study. Although the datasheet from Sigma-Aldrich indicates that its average molecular weight is about 92000 base pairs (bps) as an unconfirmed data it was independently measured in this study after purchase using electrophoresis measurement and it has been determined to be about 8 million Daltons (8000 kDa) - 12,000 bps/molecule (Figure 2.1).

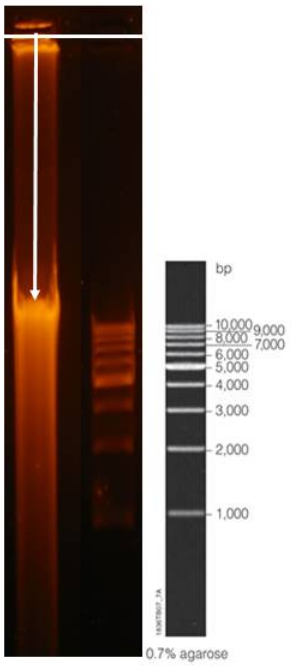

Figure 2.1: DNA molecular weight conformation by electrophoresis measurement. DNA is at the left lane and marker is at the right lane. The top white line is the start line basing on the molecular weight DNA will travel different distance and by comparing to the marker (right lane and data sheet) the molecular weight of our DNA is about 12000 Base pairs (bps).

For the preparation of the DNA thin-film device, the aqueous solution of the natural DNA was first prepared by dissolving 1 g of the DNA in 250 ml of deionized water at room temperature, and the film was drop-casted on a substrate with electrodes. In order to generate DNA thin-films with less hydrophilicity for comparison, the counterion – Na in this study – of the natural DNA was replaced with hexadecyltrimethylammonium-chloride (CTMA) to form DNA-CTMA complex (Figure 2.2).The complex was made by mixing the natural DNA solution and the aqueous solution of CTMA solution (4g/L) at room temperature. stirring for 4 hours. Once the complex was precipitated, it was vacuum-filtered and placed in the vacuum chamber drying up for 24 hours. For its thin-film deposition, the complex was dissolved in butanol with the weight concentration of 4g/ L and the DNA-CTMA complex film was drop-casted from the solution on to the substrate at room temperature.

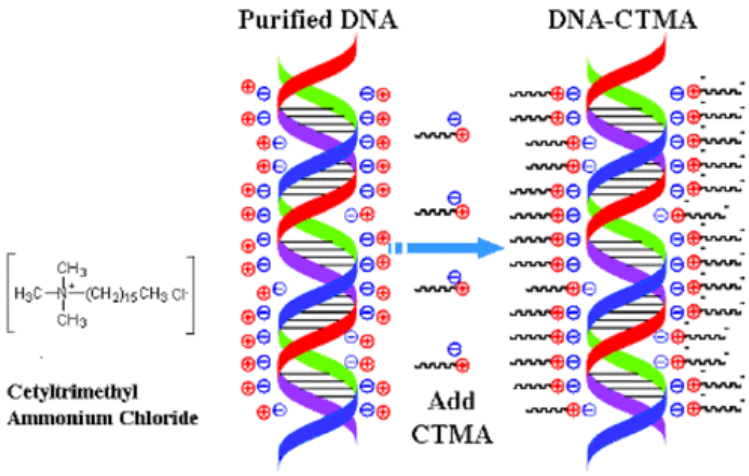

Figure 2.2: Schematic of theIon exchange reaction between Na, counterion of DNA and CTMA forming DNA-CTMA complex [62].

2.2 Electrodes and Thin Film Deposition

Oxidized silicon wafer has been chosen as a substrate for this work because of the low conductivity of SiO_2 (1 x 10^{13} Ω·m at 20^{O} C). Oxidized wafer was purchased from Wacker-Chemitronics and the thickness of SiO_2 was 1 µm. The wafer was cleaned using organic

solvents under ultrasonication for 20 minutes in each solvent. After rinsing the wafer with deionized water, it was dried - with nitrogen gas.

The deposition and the definition of the metal electrodes on top of the oxide were achieved by using a thermal evaporator (NRC 3117) (Figure 2.3(a)) and masking the wafer. Cr was deposited first with the thickness of 20 nm and the 100 nm-thick Au indicated by quartz-crystal balance inside sputter was deposited on top of Cr – Cr improves the adhesion of Au. The gap between the electrodes was about 1 mm. For the drop-casting of the DNA thin-film, 30 μl DNA solution was dropped onto the gap between the electrodes and dried under air for 12 hours (Figure 2.3(b)) – the same procedure was taken for DNA-CTMA thin-film as well. Prior to I-V measurements, all the films on the substrate were left in a vacuumed for 2 hours in order to achieve the equilibrium condition.

(a) (b)

Figure 2.3: (a) Thermal evaporator used for Cr and Au deposition to fabricate the test structure and (b).schematic of the sample used in this study.

2.3 Electrical Characterization

In order to study the effect of humidity on the conduction in DNA, a home-built humidity-control chamber (Figure 2.4) was used. It was equipped with a hygrometer (WS-7720U-IT) to measure RH and the four-point probes were placed inside chamber to obtain DC I-V characteristics. Compared to 2-point probes, four-point probes can avoid the contact resistance

by only measuring the voltage drop between two probes inside while the given (known) current was flown through two probes outside (Figure 2.5). For this study, each metal electrode has two probes contacted to set up the four-point probe configuration.

The RH was controlled by two steps. First, when the RH below the ambient RH (~ 50%) was targeted, a vacuum pump was used to evacuate the chamber. The RH was saturated typically down at 20 % after pumping constantly for 2 hours. RH was varied by controlling the valve between the chamber and the atmosphere – the humidifier was not connected in this case, and we have confirmed that a half hour waiting time was necessary to achieve the equilibrium. Secondly, when RH higher than ambient RH was targeted, both the vacuum pump and the humidifier were connected and the flow of water vapor was limited by the valve between the chamber and the humidifier. While RH was varied from RH 20% to 85%, I-V curves were measured with a voltage changing from -40 V to 40 V.

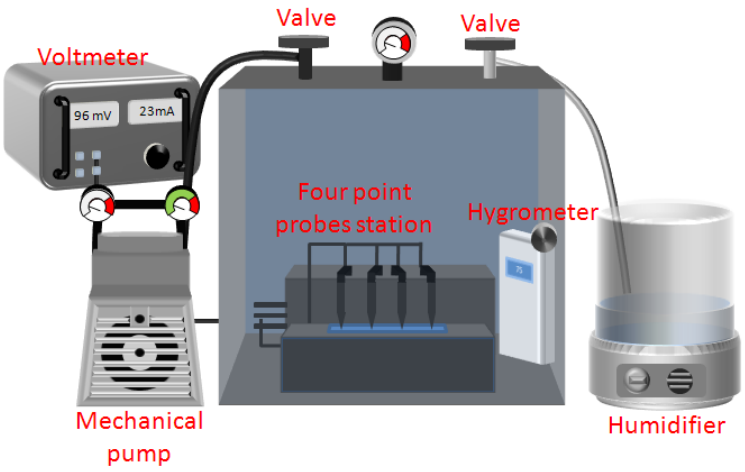

Figure 2.4: Schematic of the home-built humidity control chamber.

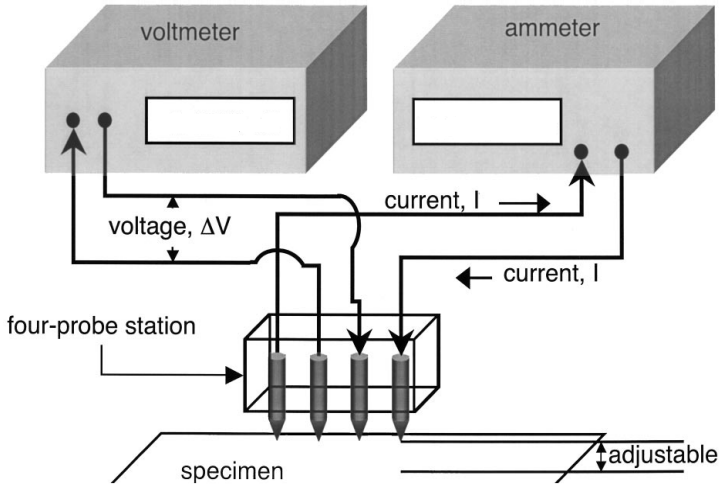

Figure 2.5: Schematic of four-point probe measurements [63].

2.4 Tomography and Element Analysis

Scanning electron microscopy (SEM) and electron energy dispersive spectrometer (EDS) were used to characterize the DNA sample after electrical measurement in order to confirm the tomography of the sample and the elements in the DNA sample after I-V measurements.

CHAPTER 3

RESULT AND DISSCUSION

3.1 Effect of Substrate during Electrical Measurements

The I-V characteristics of the oxidized Si wafer with the Au electrodes but without the DNA film was first looked at as a function of RH. The current level of the bare substrate was under 1 nA range – detection limit of the current meter regardless of the magnitude of RH. (Figure 3.1). It indicated that the conduction through the substrate was minimal compared to the conduction by DNA films when there is a DNA film between the electrodes. In addition, it should be noted that the microscope slide glass often used in many different studies have a good amount of ionic conduction and it could be as conductive as DNA when temperature is high enough. Author likes to advise other researchers to avoid using the microscope slide glass as a direct substrate to DNA when they study its electrical conductivity for the reason. Meanwhile, we have confirmed that the conduction level of the oxidized wafer used in this study stayed undetectable when the temperature was up to 100 ºC (not shown). However, this study does not aim to study the temperature effect on its conduction because the change in temperature also changes the equilibrium concentration of water in DNA complicating the analysis. In addition, it was not trivial to achieve equilibrium concentration of water content in DNA at different temperatures. Authors have a pessimistic doubt that many different studies from literature where temperature was varied to study its effect overlooked the diffusion kinetics of water in and out of DNA. Further improvement of the humidity chamber and the very precise control of the temperature would be necessary to design the experiment that could reveal the real effect of temperature and humidity on the conduction at the same time.

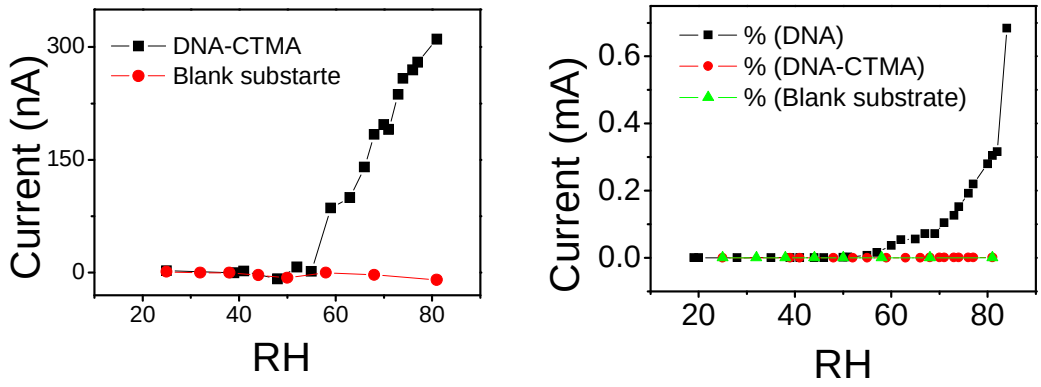

Figure 3.1: Electrical conduction of DNA film, DNA-CTMA film, and the substrate without the DNA film as a function of RH. Current was measured at 4 V.

3.2 The Effect Of RH on the I-V Characteristics of DNA and DNA-CTMA Thin-Films

The conductance started increasing at around 60% RH for both DNA and DNA-CTMA films (Figure 3.1), and the overall results are very consistent with those from previous studies by Otsuka *et al.* [12] and Kleine-Ostmann *et al.* [13]. Otsuka *et al.* has indicated that there are about 5 to 6 water molecules bound to each phosphate group in the backbone of DNA at 65% R.H where water molecules might have a chance to form a water layer around the backbone. Kleine-Ostmann *et al.* also observed the poor conduction under RH of 50 % and exponential increase in conductance with increasing RH above 60 %. Their analysis led to the speculative conclusion that water layer around the DNA backbone is self-ionized under the bias and it creates an appreciable amount of ionic (protonic) conduction via the water layer without much contribution from the electronic transport via DNA chains. While this conclusion is the most up-to-dated understanding of the effect of humidity on the long-range electrical conduction of DNA, there has not been any direct evidence of it.

DNA-CTMA film is expected to be less hydrophilic than the natural DNA because the long carbon chain in CTMA is hydrophobic and it is supposed to have a tendency to keep water molecules away from DNA backbone. In fact, conduction level in DNA-CTMA thin film was almost thousand times lower than that of DNA thin film as shown in Figure 3.1.

Full analysis of I-V characteristics from DNA (Figure 3.2) and DNA-CTMA (Figure 3.3) is as follows. First of all, both DNA and DNA-CTMA show two different regimes as RH increases - ohmic at low RH and the characteristics of the negative differential resistance (NDR) at high RH. The natural DNA, in particular clearly showed NDR when RH became over about 65 % while RH had to be quite high (over 82 %) for DNA-CTMA to start showing the weak signature of NDR.

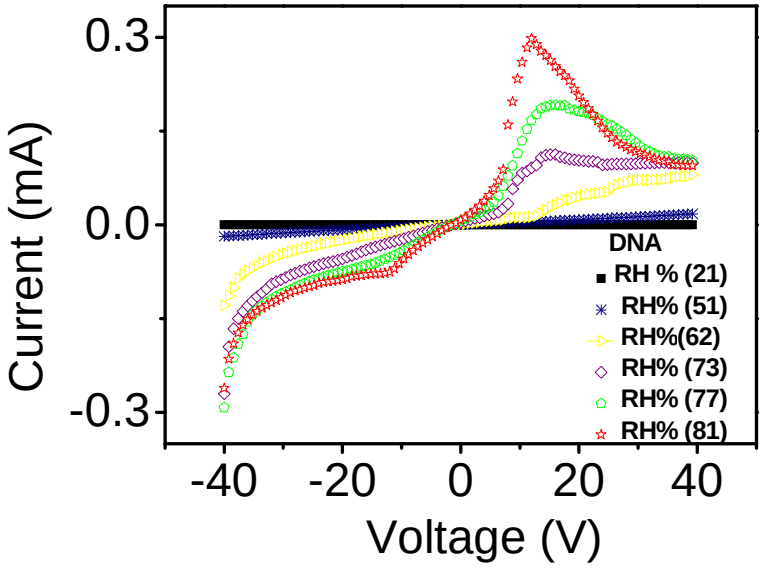

Figure 3.2: I-V curves of the natural DNA film on Au electrodes at different RH.

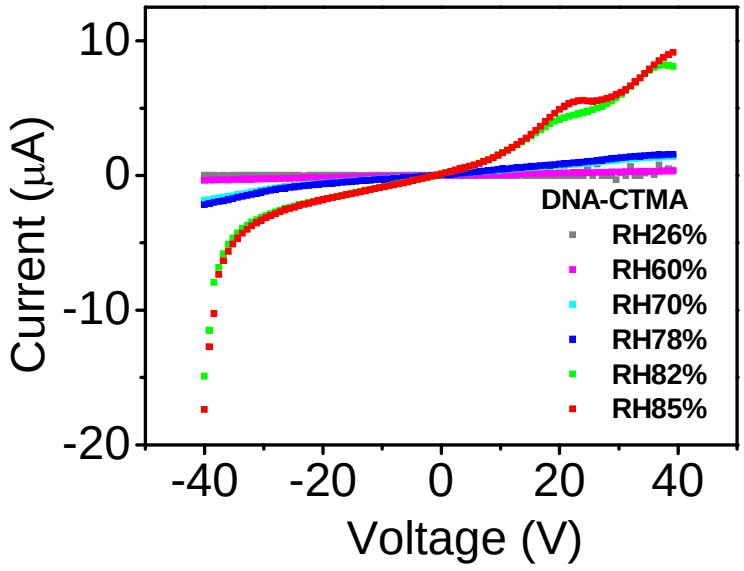

Figure 3.3: I-V curves of DNA-CTMA film on Au electrodes at different RH.

In order to understand the nature of the NDR observed before making any hasty conclusions on results from the first set of experiments, the next set of experiments were performed and their results were discussed in the following section 3.3. Author will discuss overall conduction mechanism reflected in Figures 3.2 and 3.3 in the later part of this chapter.

3.3 Negative Differential Resistance (NDR)

NDR typically implicates the current drop with an increasing applied voltage over a specific range which is commonly observed in a microelectronic devices made with highly doped semiconductor. Examples include resonant tunneling diodes [64] and Gunn diodes [65]. The basic principle of NDR in the tunnel diode is introduced in Appendix C. Recently, NDR has also been found in some organic molecules as well [66-69].The mechanisms causing NDR in the molecular systems often involve either (i) a series of reduction reactions transforming the molecule into its insulating state, which prevents further conduction,[66] (ii) a feed-limited redox reaction,[67] (iii) chemical reaction between charged molecules and ambient oxygen that produces less conductive molecules,[68] or (iv) diffusion-limited redox reaction[69]. The

examples in the literature are following.Chen *et al.* in 1999 was the first group who found a NDR characteristic out of a self-assembled organic monolayer which was made of an oligomer containing a nitroamine redox center [66]. The molecule and the mechanism for NDR is shown in (Figure 3.4). Two Au electrodes sandwich a monolayer of 2'- amino – 4– ethynylphenyl- 4' - ethynylphenyl- 5'- nitro- 1- benzenethiol, as shown in the figure. Under the forward bias, the electrons are injected from the top electrode to the polymer and the NDR is derived from two consecutive reduction reaction. At the second reduction step, the molecule becomes at its insulating state (Figure 3.4 (C)) and blocks the electron flow causing NDR.

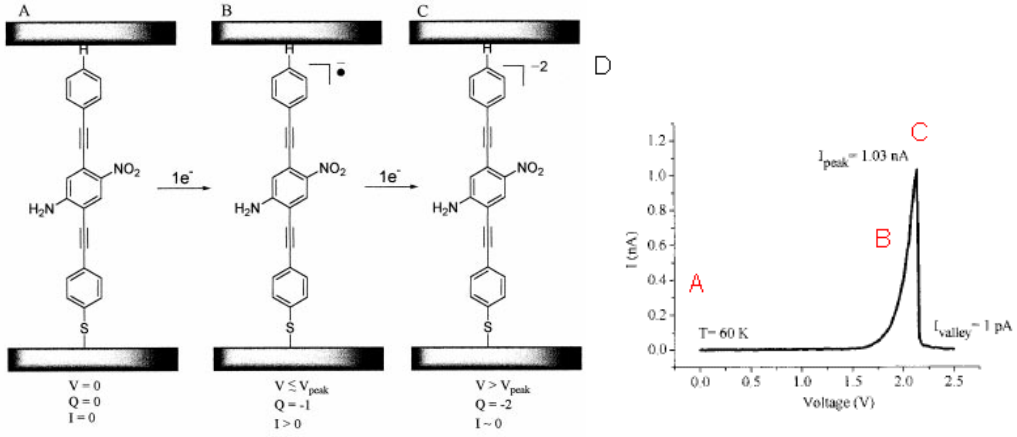

Figure 3.4: NDR observed from a monolayer of 2'-amino–4–ethynylphenyl-4'-ethynylphenyl-5'-nitro-1- benzenethiol: (A) intrinsic state of the molecule, (B) the monolayer after the first reduction, (C) insulating state of the monolayer after second reduction, and (D) I-V curve of the monolayer -the red characters are corresponding to the different states of the monolayer, A, B, and C [66].

Tang *et al.* fabricated a device with a metalloprotein with several ferritin molecules placed between electrodes (gap size: 20 nm) functionalized with carbon nanotubes (Figure 3.5(a)), and showed a feed-limited redox reaction producing NDR [67]. They concluded that the Fe(Ⅲ) in their system reduced to Fe(Ⅱ) which caused the electrons to be trapped and localized producing the characteristics of NDR. While the redox reaction in Fe ion was expected to be reversible, there was only a limited number of Fe ions in the system.

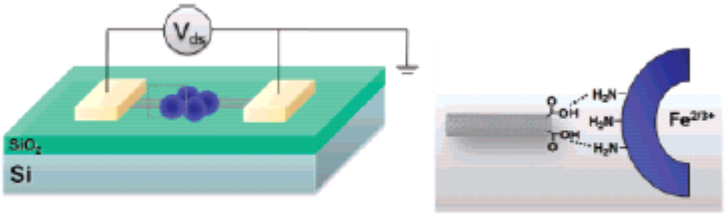

(a)

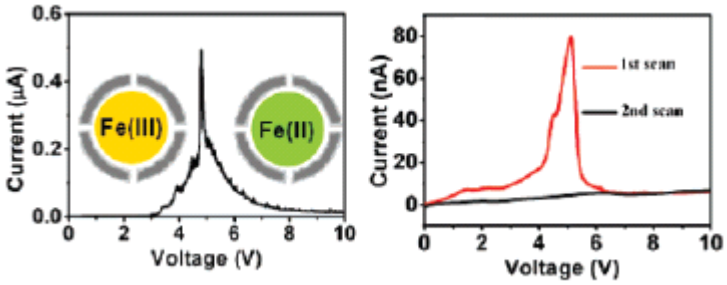

(b)

Figure 3.5: An example of NDR from a feed-limited organic redox system: (a) a NDR device made by metalloprotein and (b) I-V curve with NDR characteristics [67].

He *et al.* has fabricated self-assembled monolayer ferrocenylundecanethiol on Au electrodes [68]. They have concluded that the ferrocene under high applied bias reacted with the ambient oxygen limiting the conduction, which has created the characteristics of the NDR by observing that inconsistent NDR behavior depending on the experimental conditions related to the exposure to oxygen. The peak associated with NRD was only seen in either positive scan (Figure 3.6 (left)) or negative scan (Figure 3.6(right)) with a probability of 33 % and there was only 5 % of chance to get both positive and negative peaks in the sweep.

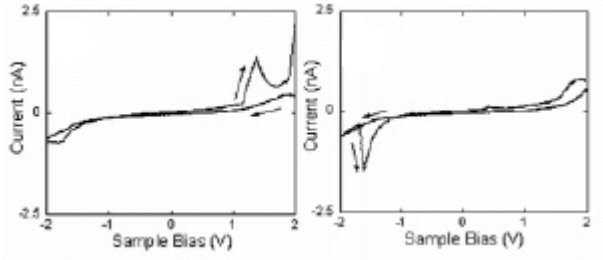

Figure 3.6: I-V characteristics of a monolayer of ferrocenylundecanethiol self-assembled on Au electrodes. The voltage was swept in different directions for the two figures; (left) - 2V → 2V→ -2V and (right) 2V → -2V→ 2V [68].

A diffusion-mediated NDR characteristic is observed in a cyclic voltammetry system [69]. The electrolysis of the reactant depletes its concentration near the electrode surface. The principle of motion of reactant is diffusion and if the reaction consumes the reactant faster than the diffusion of reactant, then a deplete region of reactant grows. Consequently, the rate of reaction decreases creating the signature of NDR.

According to the results, it can be first argued that water molecules attached to the bases in DNA promote a π- band inside the DNA double strands and the degree of conjugation is proportional to the water content over the threshold RH In an attempt to prove the fact, the set of new I-V curves were obtained by using Cu electrodes instead of Au electrode as the peak is expected to appear at lower voltage due to the lower work function of Cu than that of Au. In fact, the NDR with the threshold RH of about 65 % was again seen with a peak position at below 10 V which is clearly lower than what we have seen with Au electrodes (Figure 3.7).

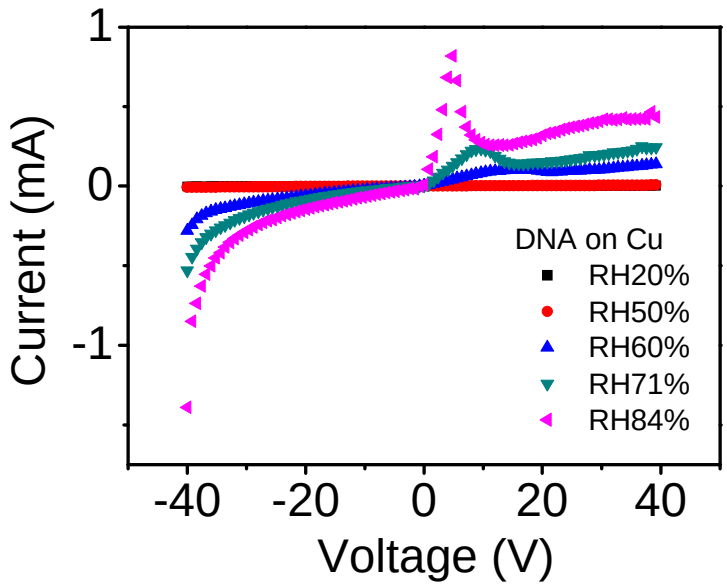

Figure 3.7: I-V curves of the natural DNA film on Cu electrodes at different RH.

However, there was a critical piece of experimental evidence that was conflict to the idea of having tunnel junction at the contact. According to the NDR from tunneling diode, it is supposed to be reproducible regardless of the voltage bias scheme. Unexpectedly, a reproducible NDR peak did not occur during the consecutive sweeps in positive voltage range from 0 V to 40 V) (Figure 3.8). It had to exclude the possibility of having tunneling junctioin at the interface between metal electrode and the hydrated DNA. Further discussion on the difference between Au and Cu electrodes can be found in the later section.

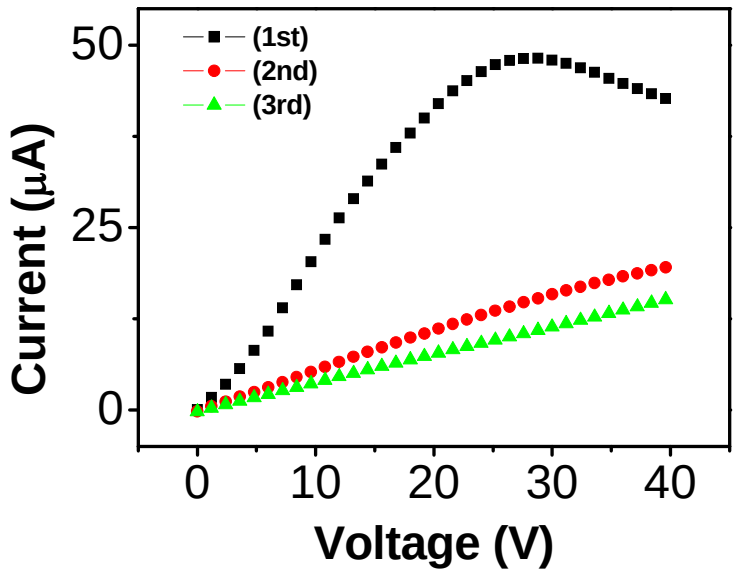

Figure 3.8: Three consecutive scans of the natural DNA thin on Au electrodes under forward bias from 0 to 40 volt.

Most examples of NDR reported for organic molecules are based on redox system as seen in the early part of this section. In fact, NDR was not often repeatable due to the permanent change in the organic systems through the redox reaction. However, further investigation of the natural DNA system showed that the NDR behavior was, in fact, reproducible as shown in Figure 3.9. This rules out any permanent change in the conductive state of the DNA molecules and the NDR would be more associated with a diffusion-limited process that is occurring in the redox system.

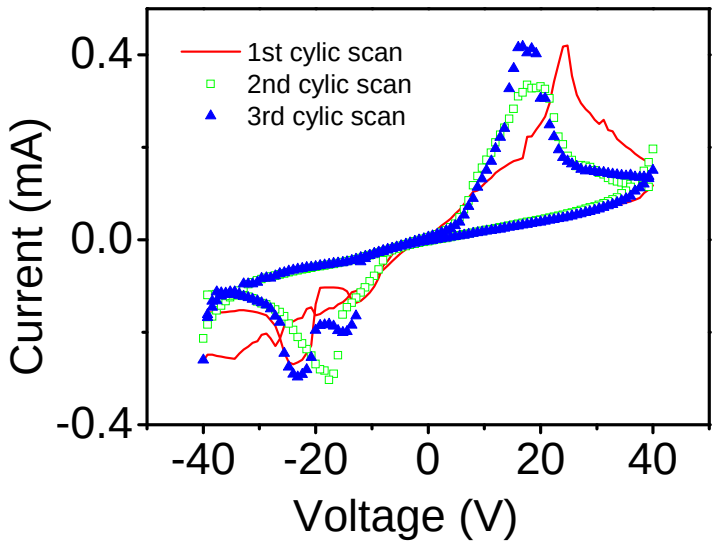

Figure 3.9: Multiple cyclic sweeps of the natural DNA sample at RH of 83%. (One cycle makes the voltage change of -40V → 40V → -40V).

3.4 NDR Mediated by Diffusion-Limited Redox Reaction in DNA

In this section, the conduction of DNA at high RH will be explained by protonic conduction caused by self-ionization of water molecules adsorbed on the DNA molecules and the NDR is attributed to the diffusion-limited process in the redox system. Meanwhile, simple ionic conduction by Na ions is ruled out because the oxidation potential of Na is very low [70] and energy dispersive X-ray analysis (EDS) did not show any accumulation of Na on the electrodes from any possible redox reaction of Na – in fact, the reduction of Na ion in water is inconceivable because neutral Na will not be stable in water. Also, author has observed the evolution of vapor at the electrodes during bias. The detailed discussion is as follows.

3.4.1 Protonic Conduction by Self-Ionized Water Molecules in DNA Thin Films

Water molecules under electrical field produce hydronium ions (H_3O^+) and hydroxide ions (OH^-) according to (3.1),

$$2H_2O(l) \rightarrow H_3O^+(aq) + OH^-(aq). \quad (3.1)$$

The potential for the ionization is known to be about 2V to 2.5V although it can change somewhat depending on the experimental configuration used [21]. Once the H_3O^+ and OH^- are created, they will drift in the electrical field and move toward anode or cathode respectively, which is called self-ionized water ionic conduction. Grotthuss published a report in 1806 and established a theory of water conductivity explaining how H_3O^+ and OH^- can move through the neutral water molecules [8]. The H_3O^+ is actually an excess proton attached on a neutral water molecule (Figure 3.10(a)), and the conduction is achieved by a proton tunneling process between water molecules bound by hydrogen bonding without any conventional long-range drift of charge carriers (ions in this case) (Figure 3.10(b)).

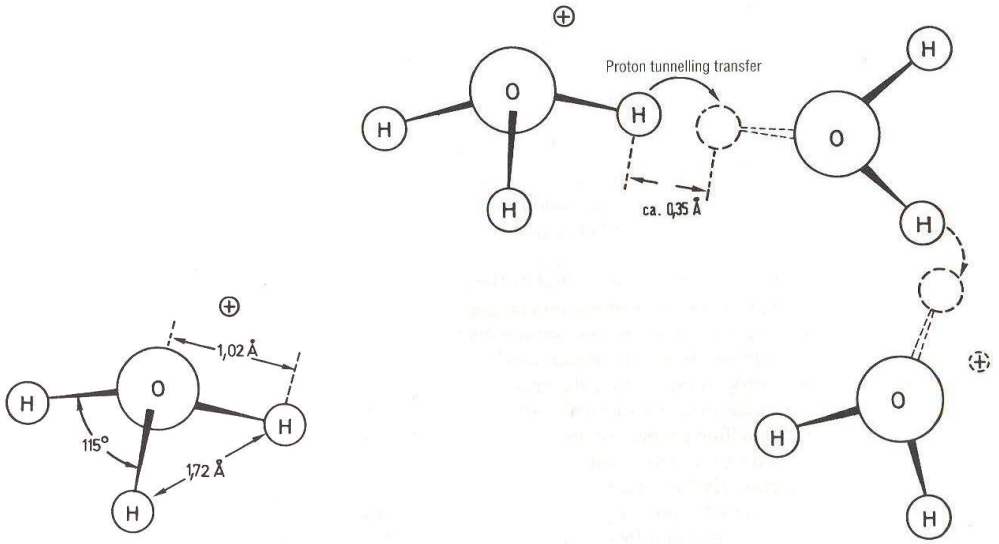

(a) (b)

Figure 3.10: Schematic of Grotthuss mechanism: (a) Structure of hydronium ion and (b) proton transport mechanism in water [21].

Based on the Grotthuss mechanism, the electrolysis of water molecules and the resulting protonic conduction in DNA thin-films are illustrated in Figure 3.11. Water molecules near the anodic Au electrode decompose to H_3O^+ and OH^-, according to reaction scheme, (3.1). The reaction at anode is,

Anode (oxidation): $2H_2O(l) \rightarrow O_2(g) + 4H^+(aq) + 4e^-$ (3.2)

The excess proton will transfer through the DNA thin film by Grotthuss mechanism and reach the cathodic Au electrode. The reaction at cathode is,

Cathode (reduction): $2H_3O^+(aq) + 2e^- \rightarrow 2H_2O(l) + H_2(g)$ (3.3)

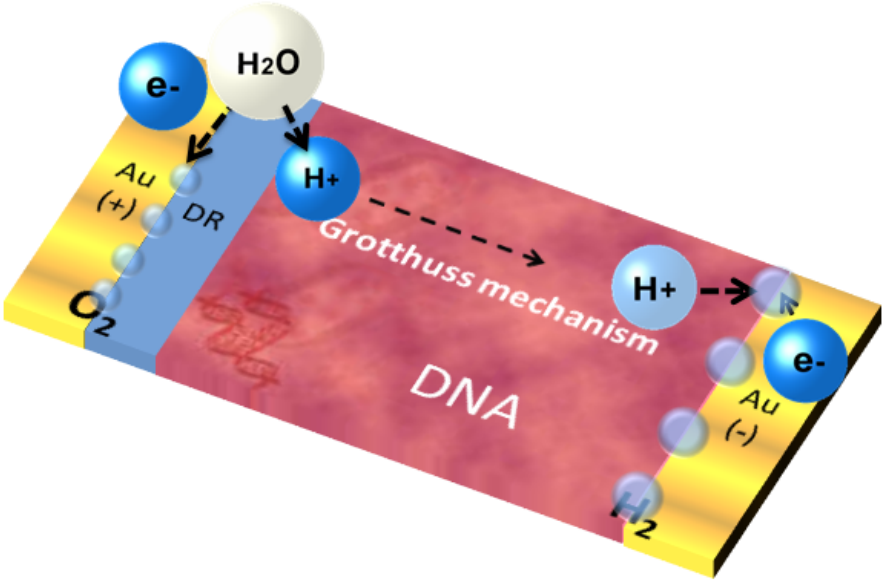

Figure 3.11: Charge transport mechanism in hydrated DNA thin-film. DR stands for deplete region of water molecules.

Figure 3.12 is a scanning electron microscope (SEM) picture of the Au electrodes after voltage sweeps. The gas evolution out of the DNA thin film left the round shape footprints of gas bubbles and they can be clear seen at the edges of Au electrodes. The gas bubbles are believed to be H_2 and O_2 and this further suggested that the electrolysis of water molecules has actually happened.

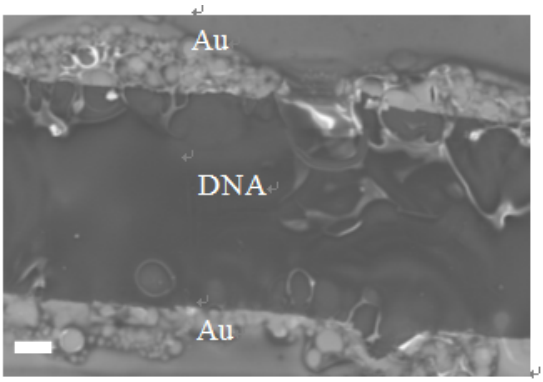

Figure 3.12: SEM picture of the DNA thin-film sample after voltage sweeps. The scale bar is 100 µm long.

3.4.2 Diffusion of Water Molecules in DNA Thin Film and NDR

Because water molecules around the anode are decomposed into oxygen gas and protons, the water concentration is expected to diminish around the anode assuming the diffusion of water molecules along the DNA chains are slower than the oxidation process at anode. This creates a deplete region (DR) of water around anode and the water molecules need to diffuse through the deplete region to reach anode for further reaction. This model could explain all the characteristics of NDR seen in the experiments so far.

For example, the signature of NDR has disappeared after consecutive positive voltage sweeps in Figure 3.8, but was repeatedly seen in full cycle of voltage sweeps in Figure 3.9. In the multiple positive sweeps, the DR was not able to disappear kinetically and kept growing scan after scan due to the limited diffusion of water, so the NDR was only seen from the first scan while ohmic conductance from the following scans was decreasing as the scan repeated. On the other hand, the DR was able to kinetically recover back to its equilibrium state in a full cycle of sweep (within about 30 sec) but created a DR at the opposite electrode and NDR at opposite bias.

If the DR in the DNA films can be refilled by water molecules fast enough, the I-V curve would not show any NDR. In fact, I-V characteristics obtained from a droplet of DI water on the

Au electrodes did not show any sign of NDR (Figure 3.13) while author has observed the gas evolution at the electrodes as the sign of electrolysis of water. This can explain that diffusion of water molecules on DNA chains is indeed much slower than self-diffusion of water.

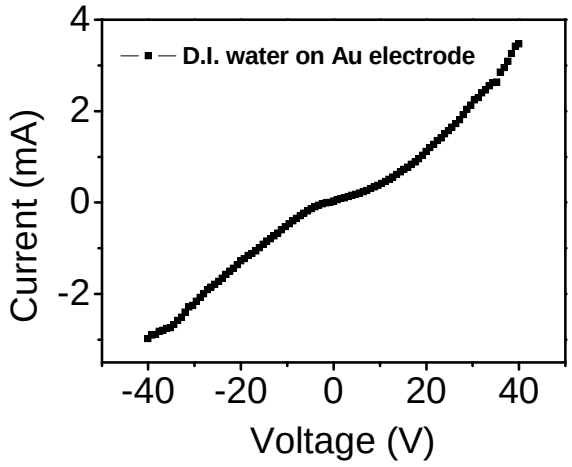

Figure 3.13: I-V characteristics of a droplet of water on Au electrodes.

3.4.3 The Effect of RH in DNA Thin-Films Revisited

First, the charge transport mechanism below the threshold RH can be suggested to be a proton (H_3O^+) hopping mechanism dominates the conduction in the DNA thin-films. With increasing RH, the proton concentration and its mobility increase as the distance between hopping sites reduces helping the charge transport.

Once RH becomes over its threshold, the water layer becomes complete around the backbone of DNA and the exponential increase in current can occur through Grotthuss conduction mechanism. The increase of the current is eventually hindered by the slow diffusion of water molecules along the DNA chains creating NDR. The difference in the threshold RH between natural DNA and DNA-CTMA is believed to be due to the difference in their hydrophilicity and Grotthuss conduction mechanism probably initiate at RH above 65 % for the natural DNA and above 80 % for DNA-CTMA thin-films.

The peak current in DNA thin film (Figure 3.2) is higher sharp with increasing RH and it can be understood because there are more water molecules in DNA and they are available for the electrolysis of water. As a result, more ions in the DNA can contribute to the conductance. While the peak position is related to both the redox potential of the system, it is also related to the kinetics associated with diffusion, charge transfer, and sweep rate. Furthermore, it could be sensitive to the bias history of the sample prior to the intended voltage sweep. Further study would be necessary to fully understand the variation of the peak position.

CHAPTER 4

CONCLUSION

The electrical property of DNA has been extensively investigated during past decade. However, the experimental outcome and the charge transport mechanisms proposed have been very scattered without clear agreement among them. Because each experiment performed in the literature has its own specific type of DNA used, the electrode configuration, different range of variables, and different environmental condition during measurement, it is extremely hard to bring out the common denominator from them to explain the unified conduction mechanism of DNA. Among the different variables, humidity has been thought as the source of long-range conduction often observed in micro/macro-scale DNA samples without clear evidence.

In this study, DNA thin films were systematically studied to reveal the picture of conduction in macro-scale DNA samples in order to probe its potential in microelectronics. From the DC I-V characteristics of the natural DNA thin-film measured in the voltage range from – 40 V to + 40 V, we have observed the exponential increase in conduction when the relative humidity became over about 65 %. The conduction below the threshold can be understood by the conventional carrier hopping conduction mechanism of the disordered materials system and the water ions are expected to be the primary carriers. For the highly hydrated natural DNA thin-films (RH over about 65 %), we have concluded that the ionized water molecules are conducting through the surface of DNA chains via proton exchange conduction mechanism (Grotthuss mechanism). The negative differential resistance caused by the limited diffusion of water molecules on DNA chains provides a clear evidence of the contribution from humidity on the long-range conduction in DNA materials.

APPENDIX A

GENERAL DC CONDUCTIVITY FROM DRUDE THEORY [71]

According to Ohm's law,

$$V = IR, \quad (1)$$

where V is potential drop along a wire, I is current flow in a wire, and R is the resistance of the wire. R depends on its dimension, but it is independent of the size of current or potential drop. In order to eliminate the dependence of R on the shape of wires, the resistivity, ρ can be introduced:

$$E = \rho j, \quad (2)$$

where E is an electric field at a specific point and j is current density that is a vector parallel to the flow of charge, and its magnitude is the amount of charge per unit time crossing a unit area perpendicular to the flow. Thus if an uniform current flows through a wire of length, L and the cross section area, A, the current density will be

$$j = I / A \quad (3)$$

Since the potential drop along the wire will be equal to EL, equation (2) will give

$$V = I \rho L / A \quad (4)$$

Since the electrical conductivity (σ) is equal to 1/ρ,

$$\sigma = I / V \bullet L / A$$

APPENDIX B

DERIVATION OF NNH AND VRH CONDUCTIVITY [27]

Nearest neighbor hopping (NNH) [27]

According to the equation (1.3) from the Chapter 1,

$V_{ij} = V_0 \exp(-2r_{ij}/\alpha) \exp\{-(|\varepsilon_i - \varepsilon_j| + |\varepsilon_i - \varepsilon_f| + |\varepsilon_j - \varepsilon_f|)/2kT\}$.

If we only consider the simplest example of hopping process, an electron hops through a system of isoenergetic sites randomly distributed in space defined by a radius of R_c with site concentration, N_0. It will be assumed that the energy sites are strongly localized and strong inequality $N_0\alpha^3 << 1$ is fulfilled. In such a case electrons will prefer to hop between nearest site and this regime. This hopping takes place when temperature is high enough so the energy term in the equation above is insignificant. Therefore the average transition rate can be expressed as follows;

$$V_{ij} = V_0 \exp(-2r_{ij}/\alpha) \quad (5)$$

By integrating over all possible distances, r_{ij},

$$\langle V \rangle = V_0 \int dr \exp(-2r/\alpha)\, 4\pi r^2 N_0 \exp(-4\pi r^3 N_0/3), \quad (6)$$

which becomes equal to $\pi V_0 N_0 \alpha^3$. (7)

Because the average number of neighboring sites available within the distance smaller than R_c can be given by

$$-4\pi R_c^3 N_0/3 = B_c \quad (8)$$

where B_c is 2.7 ± 0.1, the conductivity can be obtained by inserting R_c

However, concentration of localized states, $N_0 \equiv \exp(-2R_c/\alpha)$ (9)

R_c can get from (8) and insert N_0 into (7)

$$\sigma = (-\gamma./\alpha N_0^{1/3}), \quad (10)$$

where γ is the concentration-independent pre-exponential factor (1.73 ±0.03).

Variable range hopping (VRH) [27]

The mechanism of VRH has been proposed by Mott [24]. The main assumption of Mott's derivation is the constancy of the density of states (DOS) near the Fermi level. The derivation is as follows.

If we consider a localized energy band with the width Γ near the Fermi level and estimate the conduction provided by the electronic states within the band. The mean distance between the states, R is given by the relation,

$$g_0 R^3 \Gamma \sim 1, \tag{11}$$

where g_0 is the DOS at the Fermi level. From equation (1.3), the conduction is proportional to

$$\exp(-2R/\alpha)\exp(-\Gamma/kT). \tag{12}$$

assuming there is a maximum hopping rate with the width $\Gamma_{1/4}$,thus differential (12) will be

$$\Gamma_{1/4} \sim kT\,(T_{1/4}/T)^{1/4} \quad (kT \equiv \beta_0/g_0\alpha^3), \tag{13}$$

where β_0 is a numerical factor. Considering (11), the relation between R and Γ, the hopping length for this band becomes

$$R_{1/4} \sim \alpha(T_{1/4}/T)^{1/4} \tag{14}$$

From (11) ~(13) the conduction becomes as follows,

$$\sigma = \sigma_0 \exp\{-(\Gamma_{1/4}/T)^{1/4}\}, \tag{15}$$

which is well known Mott law.

At low temperature, $T_{1/4}$ becomes smaller than $\Gamma_{1/4}$, then the relation between Γ and R is not given by (11). The mean distance R is determined by Coulomb interaction:

$$R \sim e^2/k\Gamma \tag{16}$$

Substituting (16) into (11) finds that the width of the band providing the maximum conduction is

$$\Gamma_{1/2} \sim kT\,(T_{1/2}/T)^{1/2} \qquad (kT \equiv \beta\, e^2/k\alpha), \tag{17}$$

where β is the numerical factor. From equations (12), (15), and (16),

$$R_{1/2} \sim \alpha(T_{1/2}/T)^{1/2} \tag{18}$$

and the conductivity obeys the following

$$\sigma = \exp\{-(T_{1/2}/T)^{1/2}\}. \quad (19)$$

APPENDIX C

NEGATIVE DIFFERENTIAL RESISTANCE (NDR) IN TUNNELING DIODE [72]

Shottky and Ohmic Junctions

Metal-n-type semiconductor junctions are often form either Shottky or Ohmic junction. When the metal work function, Φ_M is larger than that of the semiconductor work function, Φ_S, the junction becomes Shottky. On the other hand, when $\Phi_M < \Phi_S$, the junction becomes Ohmic. For reader information, if it is metal p-type semiconductor junction, the situation is just opposite.

Shottky Junction

Shottky junction with n-type semiconductor is graphically shown in Figure 1 as an example. When they contact, the electrons will diffuse from semiconductor to metal because metal has lower energy states for electrons and it will continue until the potential difference stops further diffusion.

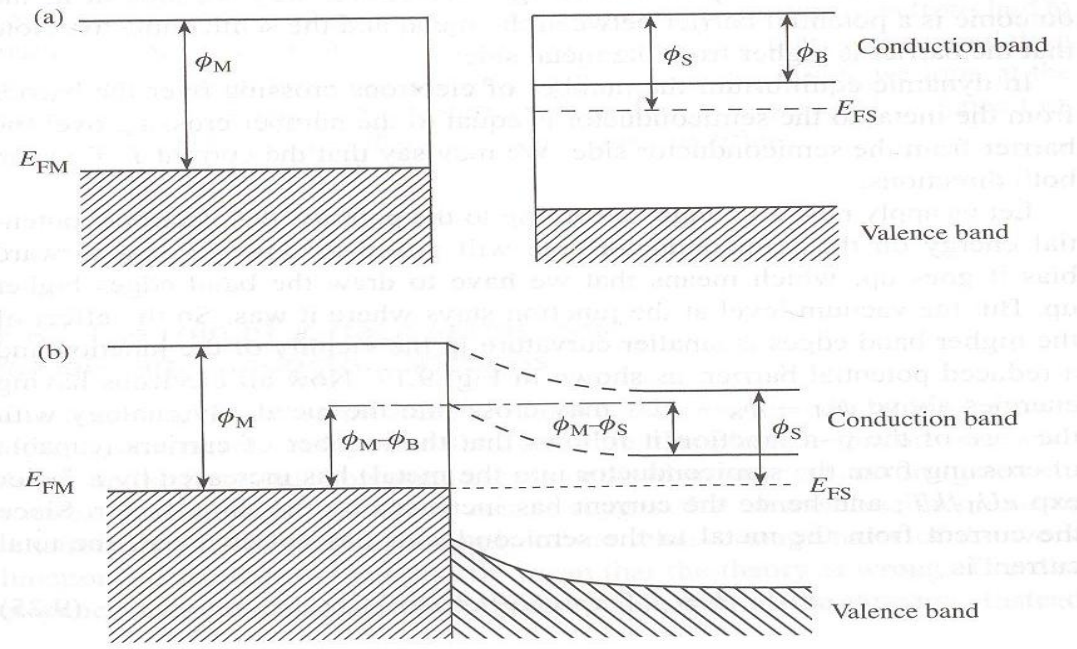

Figure 1: Energy diagram between metal and n-type semiconductor ($\Phi_M > \Phi_S$), (a) before and (b) after contact [72].

The semiconductor band will bend as described in Figure 1(b) resulting in an energy barrier. The energy diagrams under bias are shown in Figure 2(b), and the overall I-V curve of a typical Schottky junction is shown in Figure 2(a).

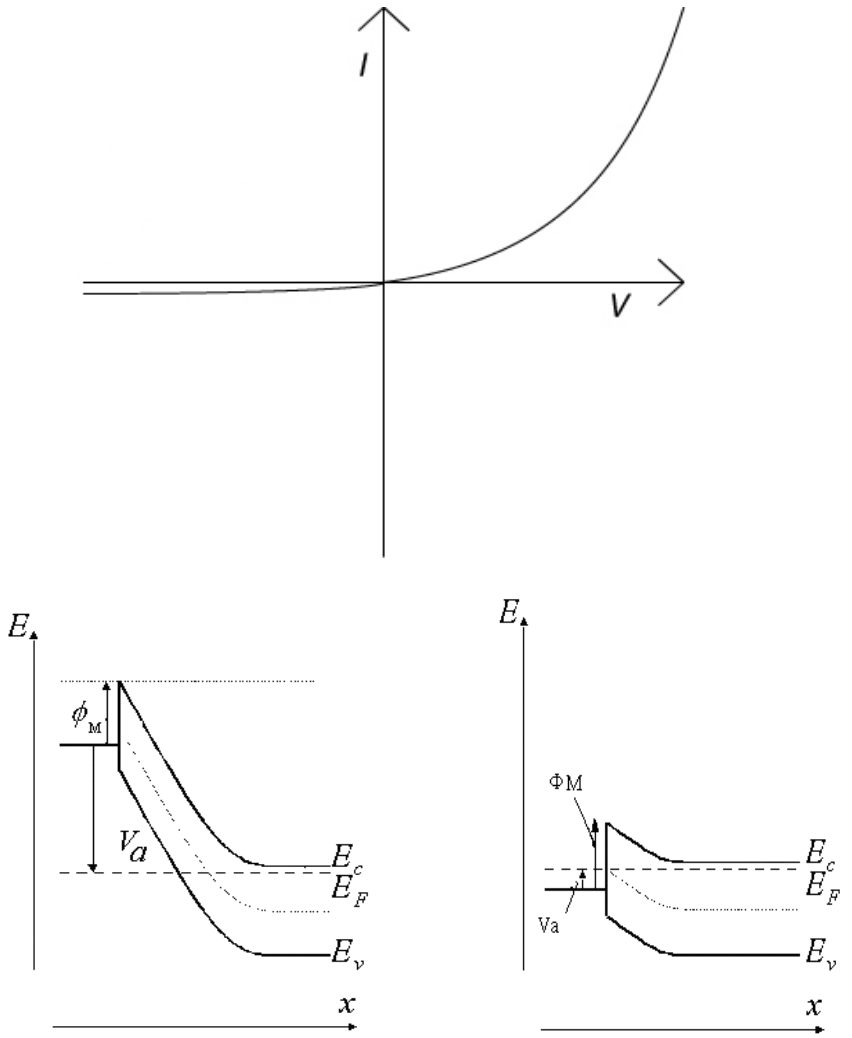

Figure 2: I-V characteristic of Schottky junction: the energy band diagrams under forward and reverse bias are plotted underneath its I-V characteristics[72].

I-V characteristic of Schottky junction is often called rectifier characteristic. Under an applied voltage, the electrons' potential energy of semiconductor is going up and down. Under a forward bias, the energy barrier becomes lower and more electrons can flow across into the metal. On the other hand, a reverse bias increases the potential barrier of the junction and the diffusion current can not occur much. However, an insignificant amount of voltage-independent current can be seen in negative part of I-V curve which is caused by the drift of carriers generated in the depletion region of the semiconductor.

Ohmic Junction

As shown in Figure 3, the electrons will diffuse from metal to the n-type semiconductor upon contact and form a band-bending region in semiconductor.

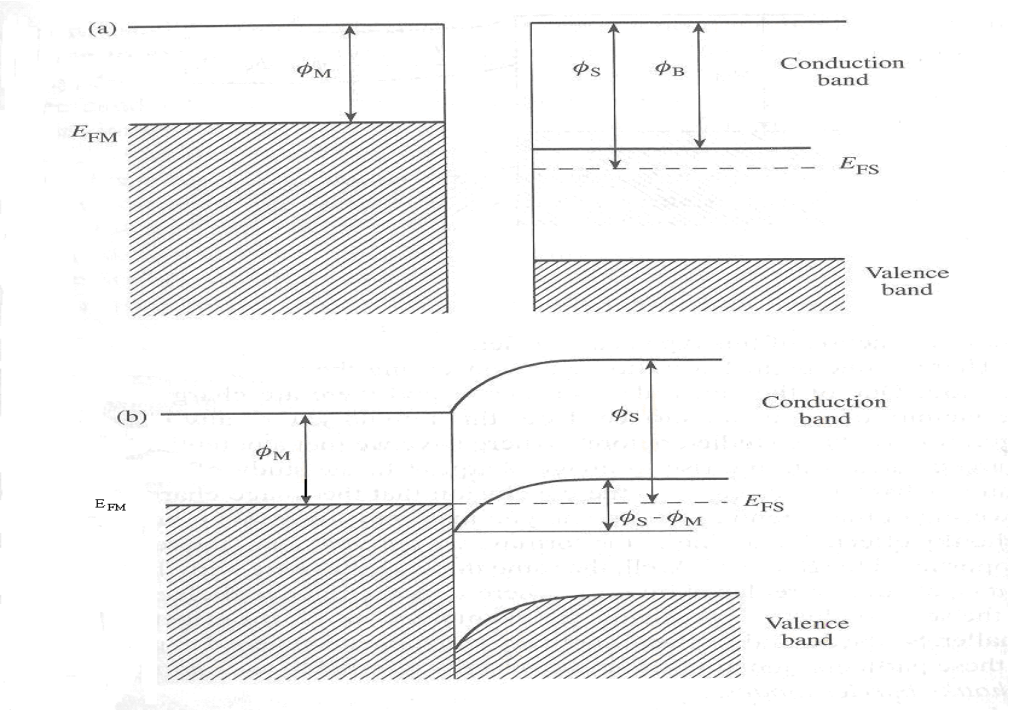

Figure 3: Energy diagram of an Ohmic junction ($\Phi_M < \Phi_S$) (a) before and (b) after contact [72].

Tunnel Diode and Negative Resistance

When the semiconductor is highly doped, the Fermi energy level is possibly moving up into the conduction band (for n-type). Under this condition, the tunnel diode happens. As shown in Figure 4, the Fermi levels of metal and semiconductor can be assumed to be similar at thermal equilibrium without bias. Under a reverse bias, the potential barrier is getting larger and the spatial distance of the depletion region is becoming smaller, so the electrons will have a chance to tunnel through the depletion region. Under a forward bias, the electrons from the highly doped n-type semiconductor might have a chance to tunnel through the depletion region to the metal. The tunnel current will have a maximum when the conduction band edge is equal

to the metal's Fermi level because it gives the extreme amount of free electrons in the semiconductor side. With further increase in the forward bias, the increasing tunnel distance makes the tunnel current less likely to happen and the electrons have to climb over the potential barrier to the metal side. Therefore a rectifier characteristic appears again.

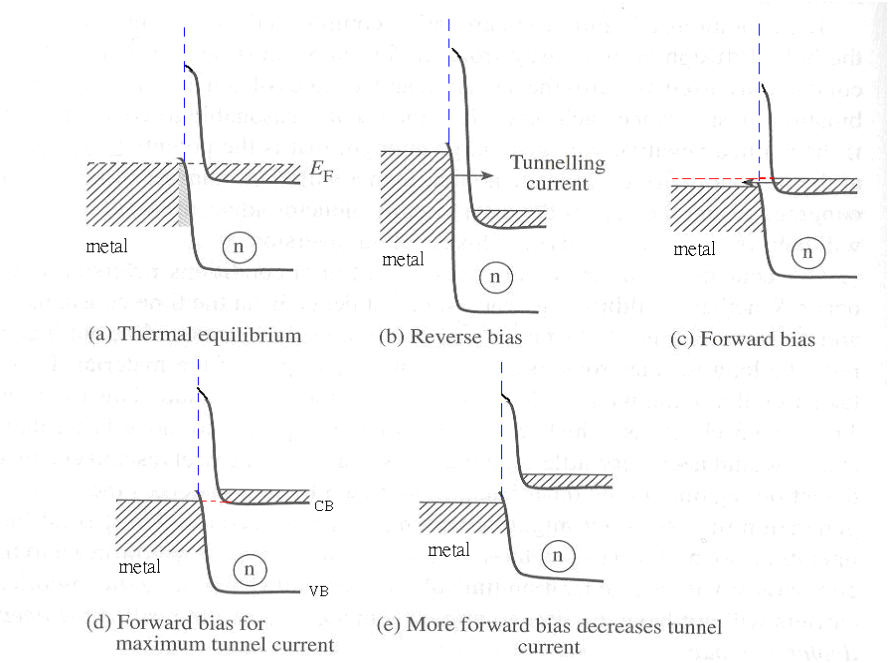

Figure 4: Energy diagram of a metal-n-type semiconductor tunnel diode [72].

Base on the discussion, its I-V curve can be plotted as Figure 6. Figure 6(a) shows the component of rectifying behavior and Figure 6(b) shows the contribution from the tunnel current, which has a maximum peak and decreasing with a increasing forward bias. By adding up both currents, we can construct the total current in the tunnel diode (Figure 6(c)). The negative slope region in the I-V curve is called negative differential resistance.

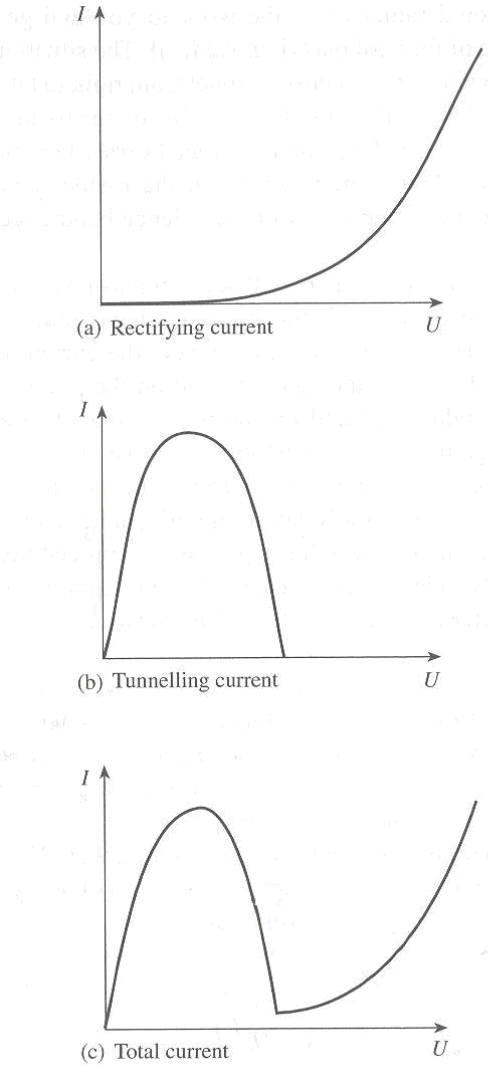

Figure 5: I-V characteristics of a tunnel diode: The total current (c) is the sum of (a) rectifier current and (b) tunneling current [72].

REFERENCES

1. Tran, P., B. Alavi, and G. Gruner, *Charge transport along the lambda-DNA double helix.* Physical Review Letters, 2000. **85**(7): p. 1564-1567.
2. Watson, J.D. and F.H. Crick, *Molecular structure of nucleic acids; a structure for deoxyribose nucleic acid.* Nature, 1953. **171**(4356): p. 737-8.
3. Seeman, N.C., *DNA in a material world.* Nature, 2003. **421**(6921): p. 427-431.
4. Storm, A.J., et al., *Insulating behavior for DNA molecules between nanoelectrodes at the 100 nm length scale.* Applied Physics Letters, 2001. **79**(23): p. 3881-3883.
5. Porath, D., et al., *Direct measurement of electrical transport through DNA molecules.* Nature, 2000. **403**(6770): p. 635-638.
6. Kasumov, A.Y., et al., *Proximity-induced superconductivity in DNA.* Science, 2001. **291**(5502): p. 280-282.
7. Murphy, C.J., et al., *LONG-RANGE PHOTOINDUCED ELECTRON-TRANSFER THROUGH A DNA HELIX.* Science, 1993. **262**(5136): p. 1025-1029.
8. Bixon, M., et al., *Long-range charge hopping in DNA.* Proceedings of the National Academy of Sciences of the United States of America, 1999. **96**(21): p. 11713-11716.
9. Schuster, G.B., *Long-range charge transfer in DNA: Transient structural distortions control the distance dependence.* Accounts of Chemical Research, 2000. **33**(4): p. 253-260.
10. Conwell, E.M. and S.V. Rakhmanova, *Polarons in DNA.* Proceedings of the National Academy of Sciences of the United States of America, 2000. **97**(9): p. 4556-4560.
11. Ha, D.H., et al., *Humidity effects on the conductance of the assembly of DNA molecules.* Chemical Physics Letters, 2002. **355**(5-6): p. 405-409.

12. Otsuka, Y., et al., *Influence of humidity on the electrical conductivity of synthesized DNA film on nanogap electrode.* Japanese Journal of Applied Physics Part 1-Regular Papers Short Notes & Review Papers, 2002. **41**(2A): p. 891-894.

13. Kleine-Ostmann, T., et al., *Conductivity of single-stranded and double-stranded deoxyribose nucleic acid under ambient conditions: The dominance of water.* Applied Physics Letters, 2006. **88**(10): p. 3.

14. Kwon, Y.W., et al., *Materials science of DNA.* Journal of Materials Chemistry, 2009. **19**(10): p. 1353-1380.

15. Mandelkern, M., et al., *THE DIMENSIONS OF DNA IN SOLUTION.* Journal of Molecular Biology, 1981. **152**(1): p. 153-161.

16. W. Cochran, F.H.C.a.V.V., *The structure of synthetic polypeptides. I. The transform of atoms on a helix.* Acta Cryst., 1952. **5**: p. 581-586

17. <http://www.bio.miami.edu/dana/104/DNA1.jpg>.

18. Yang, S.T., et al., *PML-dependent apoptosis after DNA damage is regulated by the checkpoint kinase hCds1/Chk2.* Nature Cell Biology, 2002. **4**(11): p. 865-870.

19. Endres, R.G., D.L. Cox, and R.R.P. Singh. *Colloquium: The quest for high-conductance DNA*. Reviews of Modern Physics [Review] 2004 Jan [cited 76 1]; 195-214]. Available from: <Go to ISI>://000220001400005.

20. R. Koradi, M.B., and K. W. Thrich, *J. Mol. Graphics*, 1996. **14**: p. 51.

21. C. H. Hamann, A.H., W. Vielstich, *Electrochemistry.* 1998.

22. Anderson, P.W., *Absence of Diffusion in Certain Random Lattices.* Phys. Rev., 1958. **109**: p. 1492 - 1505

23. Twose, N.F.M.a.W.D., *Adv. Phys.*, 1961. **10**: p. 107.

24. Mott, N.F., *Phil. Mag.*, 1970. **22**: p. 7.

25. Davis, N.F.M.a.E.A., *Electronic Processes in Non-Crystalline Materials, 2nd Edition, Clarendon, Oxford.* 1979.

26. Siegner, U., et al., *OPTICAL DEPHASING IN SEMICONDUCTOR MIXED-CRYSTALS.* Physical Review B, 1992. **46**(8): p. 4564-4581.

27. Baranovski, S., *Charge Transport in Disordered Solids, Wiley & sons, Ltd* 2006.

28. Lakhno, V.D. *DNA nanobioelectronics*. 2008: John Wiley & Sons Inc.

29. Duchesne, J., et al., *Thermal and electrical properties of nucleic acids and proteins.* Nature, 1960. **188**: p. 405-6.

30. Jortner, J., et al., *Charge transfer and transport in DNA.* Proceedings of the National Academy of Sciences of the United States of America, 1998. **95**(22): p. 12759-12765.

31. Fink, H.W. and C. Schonenberger, *Electrical conduction through DNA molecules.* Nature, 1999. **398**(6726): p. 407-410.

32. Bellido, E.P., et al., *Current-voltage-temperature characteristics of DNA origami.* Nanotechnology, 2009. **20**(17): p. 175102.

33. Kutnjak, Z., et al., *Electrical conduction in native deoxyribonucleic acid: Hole hopping transfer mechanism?* Physical Review Letters, 2003. **90**(9): p. 4.

34. Yoo, K.H., et al., *Electrical conduction through poly(dA)-poly(dT) and poly(dG)-poly(dC) DNA molecules.* Phys Rev Lett, 2001. **87**(19): p. 198102.

35. Tessler, N., et al., *Charge Transport in Disordered Organic Materials and Its Relevance to Thin-Film Devices: A Tutorial Review.* Advanced Materials, 2009. **21**(27): p. 2741-2761.

36. Kutnjak, Z., et al., *Electrical conduction in macroscopically oriented deoxyribonucleic and hyaluronic acid samples.* Physical Review E, 2005. **71**(4): p. 8.

37. Yu, Z.G. and X.Y. Song, *Variable range hopping and electrical conductivity along the DNA double helix.* Physical Review Letters, 2001. **86**(26): p. 6018-6021.

38. *http://physicsworld.com/cws/article/print/60*.

39. Lewis, F.D., et al., *Crossover from superexchange to hopping as the mechanism for photoinduced charge transfer in DNA hairpin conjugates.* Journal of the American Chemical Society, 2006. **128**(3): p. 791-800.

40. Braun, E., et al., *DNA-templated assembly and electrode attachment of a conducting silver wire.* Nature, 1998. **391**(6669): p. 775-778.

41. Rakitin, A., et al., *Metallic conduction through engineered DNA: DNA nanoelectronic building blocks.* Physical Review Letters, 2001. **86**(16): p. 3670-3673.

42. Cai, L.T., H. Tabata, and T. Kawai, *Self-assembled DNA networks and their electrical conductivity.* Applied Physics Letters, 2000. **77**(19): p. 3105-3106.

43. Dulic, D., et al., *Direct conductance measurements of short single DNA molecules in dry conditions.* Nanotechnology, 2009. **20**(11): p. 115502.

44. Zhang, Y., et al., *Insulating behavior of lambda-DNA on the micron scale.* Physical Review Letters, 2002. **89**(19): p. 4.

45. W.Saenger, *Principle of Nucleic Acid Structure; Springer -Verlag, New York 1984 p.556.*

46. Franklin, R.E. and R.G. Gosling, *Molecular configuration in sodium thymonucleate.* Nature, 1953. **171**(4356): p. 740-1.

47. Q. Zhen, D.K., X. Gao, S. Xie, Front. Phys. China, 2008. **3**: p. 349.

48. Robinson, C.R. and S.G. Sligar, *MOLECULAR RECOGNITION MEDIATED BY BOUND WATER - A MECHANISM FOR STAR ACTIVITY OF THE RESTRICTION-ENDONUCLEASE ECORI.* Journal of Molecular Biology, 1993. **234**(2): p. 302-306.

49. Feig, M. and B.M. Pettitt, *A molecular simulation picture of DNA hydration around A- and B-DNA.* Biopolymers, 1998. **48**(4): p. 199-209.

50. Berashevich, J. and T. Chakraborty, *Water induced weakly bound electrons in DNA.* Journal of Chemical Physics, 2008. **128**(23): p. 6.

51. Berashevich, J. and T. Chakraborty, *How the Surrounding Water Changes the Electronic and Magnetic Properties of DNA.* Journal of Physical Chemistry B, 2008. **112**(44): p. 14083-14089.

52. Prive, G.G., et al., *HELIX GEOMETRY, HYDRATION, AND G.A MISMATCH IN A B-DNA DECAMER.* Science, 1987. **238**(4826): p. 498-504.

53. Jo, Y.S., Y. Lee, and Y. Roh, *Effects of humidity on the electrical conduction of lambda-DNA trapped on a nano-gap Au electrode.* Journal of the Korean Physical Society, 2003. **43**(5): p. 909-913.

54. Tuukkanen, S., et al., *Dielectrophoresis of nanoscale double-stranded DNA and humidity effects on its electrical conductivity.* Applied Physics Letters, 2005. **87**(18): p. 3.

55. Armitage, N.P., M. Briman, and G. Gruner. *Charge transfer and charge transport on the double helix*. 2004: Wiley-V C H Verlag Gmbh.

56. Tanaka, K., et al., *Ionic conduction in glasses.* Physica Status Solidi a-Applied Research, 1999. **173**(2): p. 317-322.

57. Angell, C.A., *MOBILE IONS IN AMORPHOUS SOLIDS.* Annual Review of Physical Chemistry, 1992. **43**: p. 693-717.

58. Ronne, C., et al., *Investigation of the temperature dependence of dielectric relaxation in liquid water by THz reflection spectroscopy and molecular dynamics simulation.* Journal of Chemical Physics, 1997. **107**(14): p. 5319-5331.

59. Debye, P., Verh. dt. phys. Ges, 1913. **15**: p. 777.

60. A. Miller, a.E.A., Phys. Rev. , 1960. **120**.

61. Okahata, Y., et al., *Anisotropic electric conductivity in an aligned DNA cast film.* Journal of the American Chemical Society, 1998. **120**(24): p. 6165-6166.

62. *http://www.lios.at/Publications/thesis/thesis-stadler.pdf.*

63. Wang, C.W., K.A. Cook, and A.M. Sastry, *Conduction in multiphase particulate/fibrous networks - Simulations and experiments on Li-ion anodes.* Journal of the Electrochemical Society, 2003. **150**(3): p. A385-A397.

64. Sollner, T., et al., *RESONANT TUNNELING THROUGH QUANTUM WELLS AT FREQUENCIES UP TO 2.5 THZ.* Applied Physics Letters, 1983. **43**(6): p. 588-590.

65. Alekseev, E. and D. Pavlidis, *Large-signal microwave performance of GaN-based NDR diode oscillators.* Solid-State Electronics, 2000. **44**(6): p. 941-947.

66. Chen, J., et al., *Large on-off ratios and negative differential resistance in a molecular electronic device.* Science, 1999. **286**(5444): p. 1550-1552.

67. Tang, Q., et al., *Redox-mediated negative differential resistance behavior from metalloproteins connected through carbon nanotube nanogap electrodes.* Journal of the American Chemical Society, 2007. **129**(36): p. 11018-+.

68. He, J. and S.M. Lindsay, *On the mechanism of negative differential resistance in ferrocenylundecanethiol self-assembled monolayers.* Journal of the American Chemical Society, 2005. **127**(34): p. 11932-11933.

69. Mabbott, G.A., *AN INTRODUCTION TO CYCLIC VOLTAMMETRY.* Journal of Chemical Education, 1983. **60**(9): p. 697-702.

70. *http://en.wikipedia.org/wiki/Sodium.*

71. Mermin, A., *Solid State Physics, Brooks/ Cole Thomson learning, P6~ P11.* 1976.

72. L. Solymar, a.D.W., *Electrical properties of materials, Oxford 7th.* 2004.

BIOGRAPHICAL INFORMATION

Hou Kuan Lee was born in Taipei, Taiwan. In 2004, he completed his bachelor degree from the Department of Resources Engineering at National Cheng Kung University in Tainan, Taiwan.

After one and half year of military service, he joined the Department of Materials Science and Engineering at the University of Texas at Arlington in 2007 pursuing a master degree. He studied at the Photovoltaic Materials Laboratory for two years and his research area covers polymer solar cells, DNA electronics, and electrical conduction in disordered material system. After completing the master degree, he will search for a job associated with exploring new recourses that would benefit the society.